University College London

The doped-atom toolbox for quantum simulation and computation

Andrew Fisher

Quantum Connections Summer School
Högberga Gård, June 2023

Overview

- Lecture 1 (Monday)
  - The requirements for quantum gates and quantum simulation
  - Introducing the ‘doped atom toolbox’
    - Donor and acceptor states, their description by effective-mass theory
    - Implantation chemistry and its limitations
    - Comparison to artificial quantum dots
  - [Break]
  - The physics of donors, simulations of Mott insulators, molecular analogues
  - Topological states and the bulk-edge correspondence
  - 1-d topological structures with donors
  - Comparison with cold-atom approaches

Overview (continued)

- Lecture 2 (Wednesday)
  - Quantum gates and other quantum simulation results with donors
  - Need for spin-orbit interactions for TIs, examples of engineered and ‘natural’ structures
  - Spherical and non-spherical models of acceptors
  - Quantum Information Processing with acceptors – advantages (and disadvantages) of hole states
  - The honeycomb Topological Insulator
  - [Break]
  - Detection of topological states via local probes
  - Comparison with cold-atom systems

Quantum computing and quantum simulation

- Quantum computing requires:
  - A set of well defined basis states (qubits)
  - Ability to initialize to a well-defined state
  - Long decoherence times
  - Universal set of quantum gates (usually single-qubit and an entangling two-qubit operation)
  - Ability to read out the qubit state
- Quantum simulation requires:
  - A well-defined target system (typically with a simple ‘model Hamiltonian)
  - A scalable quantum system with controllable parameters whose state space and other properties can be mapped to the target system
  - A means of verifying output (e.g. the Hamiltonian simulated and/or final state)

The logic of quantum simulators

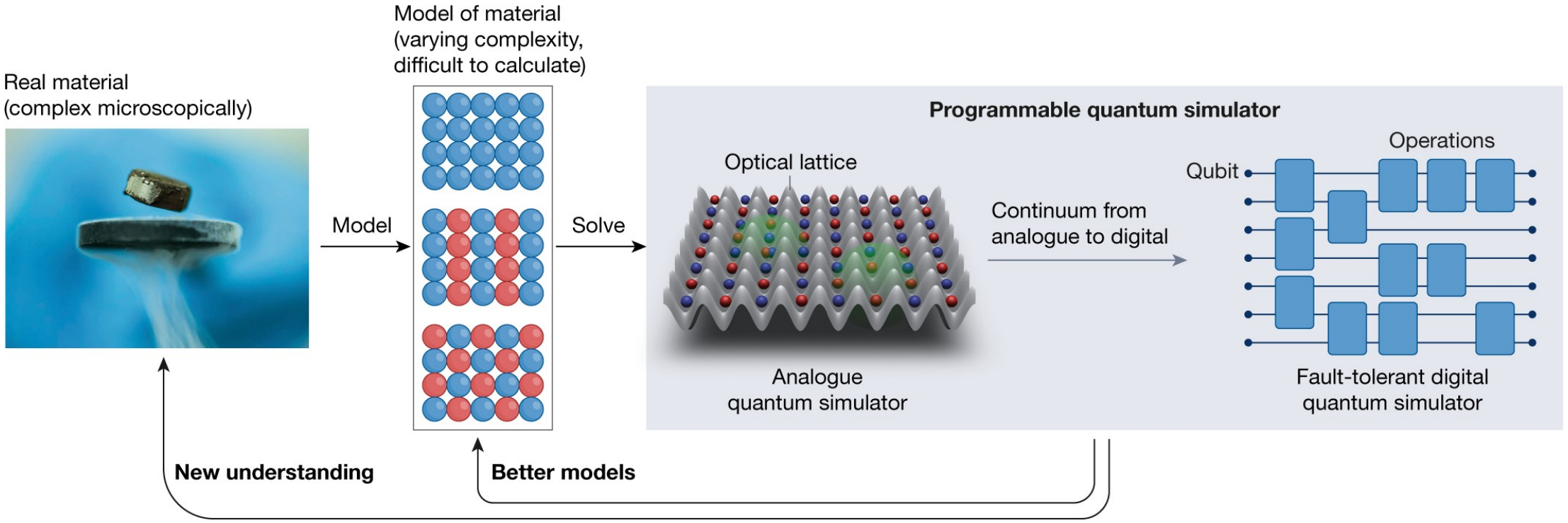

Daley *et al.* Nature **607** 667-676 (2022)

‘Digital’ and ‘analogue’ simulation

- ‘Digital’ simulation

  Apply a controlled sequence of gates to represent unitary dynamics

$$\hat{U} = \exp\left(\mathrm{i}\hat{H}\delta t/\hbar\right) = \prod_l \exp\left(\mathrm{i}\hat{H}_l\delta t/\hbar\right) + \text{corrections}$$

  With full fault tolerance, only remaining source of error is Trotter error from time slicing

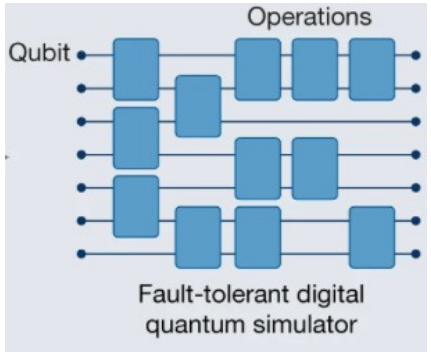

- ‘Analogue’ simulation

  Find mapping from (usually low-energy) state space of physical system to the model Hilbert space

  Arrange ‘natural’ interactions to match those in the desired model

  Prepare initial state and carry out evolution in (continuous) time

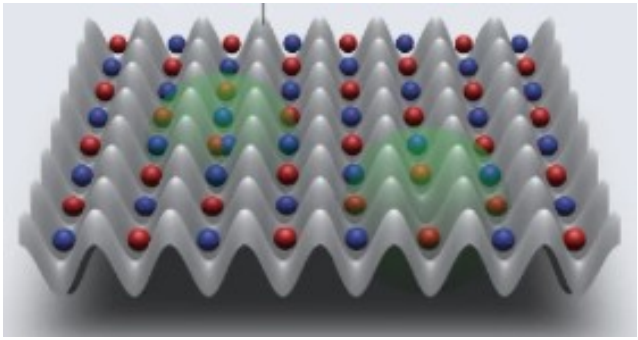

Outputs and verification

State tomography: seek full characterization of *state* (exponential classical effort, or comparison with reference state via quantum teleportation)

N-qubit state → -1 measurements (or perfect 2*N*-qubit entangled state for teleportation and comparison)

Classical shadows: random state rotation, then measurement in computational basis to give a bit string

$$\hat{\rho} \rightarrow \langle \vec{b}|\hat{U}\hat{\rho}\hat{U}^{\dagger}|\vec{b}\rangle \quad \text{with} \quad \mathbb{E}\left[\hat{U}^{\dagger}|\vec{b}\rangle\langle\vec{b}|\hat{U}\right] = \mathcal{M}(\hat{\rho}) \quad \Rightarrow \quad \hat{\rho} = \mathcal{M}^{-1}\mathbb{E}\left[\hat{U}^{\dagger}|\vec{b}\rangle\langle\vec{b}|\hat{U}\right]$$

Sample of *N* such results (the 'shadow' of the state) gives unbiased estimator and efficient predictions of *M* linear targets via a 'median of means' approach:

$$\mathrm{Tr}[\hat{O}_1\hat{\rho}]\ldots\mathrm{Tr}[\hat{O}_M\hat{\rho}] \quad \text{with additive error provided} \quad N \geq \mathcal{O}\left(\frac{\log(M)\max_i ||\hat{O}_i||^2_{\mathrm{shadow}}}{\epsilon^2}\right)$$

(optimal scaling)

Relevant operator norm is strongly constrained for local targets: for support on *k* qubits

$$||\hat{O}_i||^2_{\mathrm{shadow}} \leq 4^k ||\hat{O}_i||^2_{\infty} \quad (\text{or } 3^k ||\hat{O}_i||^2_{\infty} \text{ for products of } k \text{ single-qubit observables})$$

Scales exponentially in *k* (not overall number of qubits)

Huang, Keung and Preskill *Nat. Phys.* **16** 1050 (2020)

Hamiltonian learning

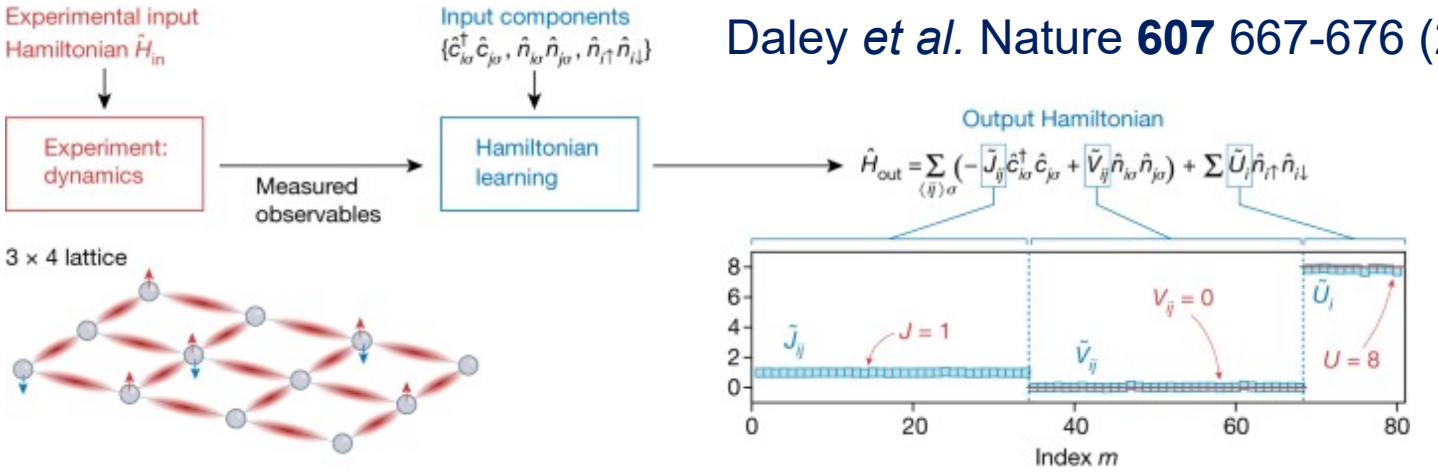

Daley *et al.* Nature **607** 667-676 (2022)

Time-independent

Expectation values of observables A having support only on L_0 in stationary states satisfy

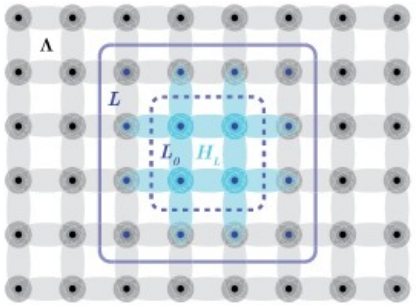

$$\langle \mathrm{i}[\hat{A}, \hat{H}_L]\rangle = 0$$

Expand in a local basis

$$\hat{H}_L = \sum_{m=1}^{M} c_m \hat{S}_m$$

Then coefficients satisfy

$$\mathbf{K}\cdot\mathbf{c} = 0 \quad \text{with} \quad K_{nm} \equiv \langle \mathrm{i}[\hat{A}_n, \hat{S}_m]\rangle$$

Solve as N linear equations for M unknowns (typically with)

Time-dependent

Replace with time-averaged expectation values: if

$$\hat{H}(t) = \hat{H}_0 + f(t)\hat{V}$$

with $\hat{H}_{0,L} = \sum_{m=1}^{M} c_m \hat{S}_m \qquad \hat{V}_L = \sum_{m=1}^{M} c_{m+M}\hat{S}_m$

$$K_{n,m} = \frac{1}{t}\int_0^t \langle[\hat{A}_n, \hat{S}_m]\rangle \mathrm{d}t' \qquad m \le M$$

$$K_{n,m+M} = \frac{1}{t}\int_0^t \langle[\hat{A}_n, \hat{S}_m]\rangle f(t')\,\mathrm{d}t'$$

Bairey *et al. Phys. Rev. Lett.* **122** 020504 (2019)

Summary

	Classical simulation	Analogue quantum simulation	Digital quantum computing
Platforms	Classical supercomputers	Neutral atoms (optical lattices or tweezer arrays), ions, superconducting systems, quantum dots, photons and so on	Neutral atoms (optical lattices or tweezer arrays), ions, superconducting systems, quantum dots, photons and so on
Universality	Yes (up to restricted system sizes or timescales) owing to exponential scaling in time (and potentially memory)	Limited to available physical models	Yes (with error correction, requiring substantial scaling up from current systems)
Quantum advantage	No, and the cost grows exponentially with system size or simulation time	Regimes of practical quantum advantage now for real scientific problems, with potential opportunities for industrial problems	Quantum primacy for specialized tasks, awaiting practical quantum advantage and eventually fault tolerance
Solvable models	Unrestricted models through best-available classical algorithms	Specific particle (fermion or boson) Hamiltonian, spin models (qubits). Potentially, other mathematical problems that can be mapped onto these models	Wide classes of models, solved through algorithms for quantum simulation on a general purpose quantum computer
System size (present day)	Less than 50 spins computed exactly, or specialized short-time calculations for larger systems	Platform dependent up to 50–1,000 particles or spins	Around 50 noisy qubits are at present available, but no fault-tolerant digital qubits yet
Scalability (near term)	Exponentially difficult to scale to larger system sizes and longer times, except for specialized problems	Direct path to 10^3–10^4 particles within the next 2–3 years	Few hundred in NISQ devices; the next step is to bring error-corrected qubits online

Daley *et al.* Nature **607** 667-676 (2022)

Some example systems

Cold atoms

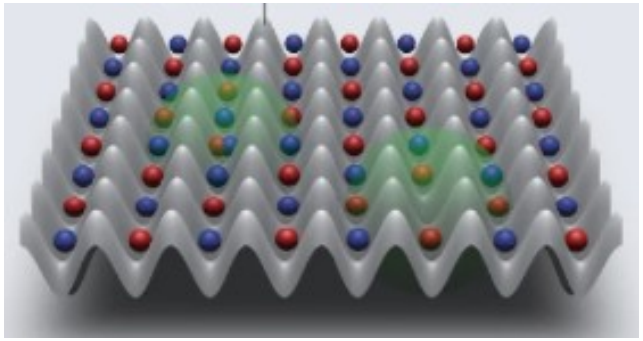

Rydberg atoms

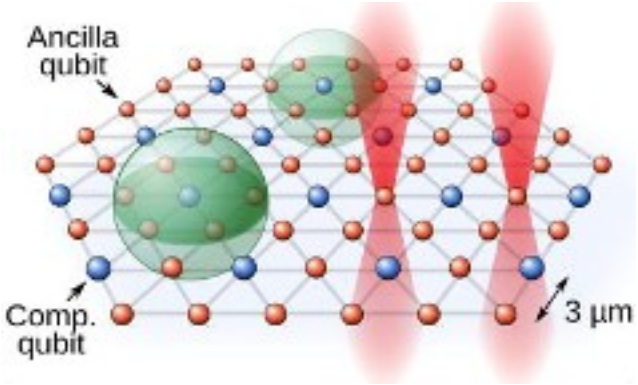

Superconducting circuits

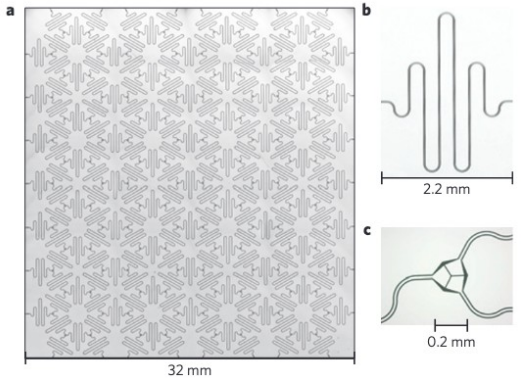

Ion traps

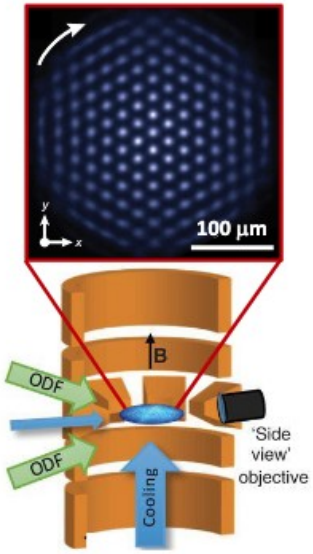

Linear optics

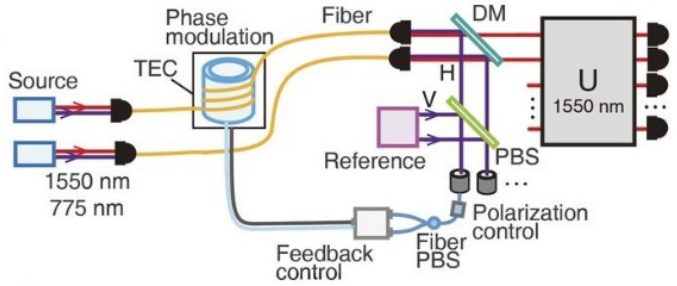

An alternative system (these lectures)

- Donors and acceptors in simple semiconductors
- In simple cases, form ‘shallow donors’ or ‘shallow acceptors’ where an additional positive (or negative) nuclear charge weakly binds an additional electron (or hole)
- Choose Si as host material because of
  - Existing material processing technologies
  - Low density of nuclear spins (natural Si is only 4.7% ^{29}Si)

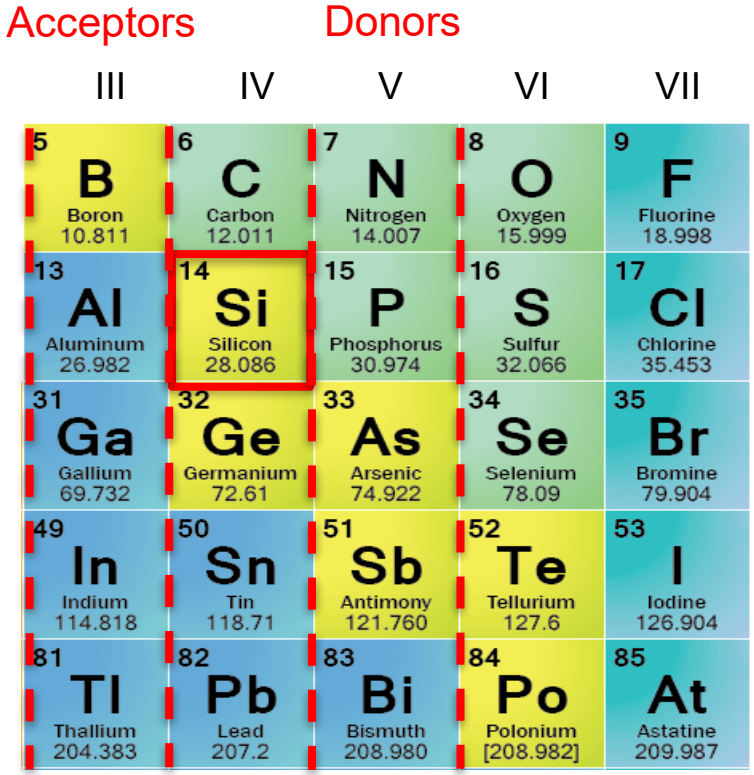

Si Quantum Information & Atomic Precise Doping

- Kane scalable quantum computer in silicon
- isolated ^{31}P nuclear spin qubits

- **isolate donors ~20 nm apart, ~20 nm below surface**

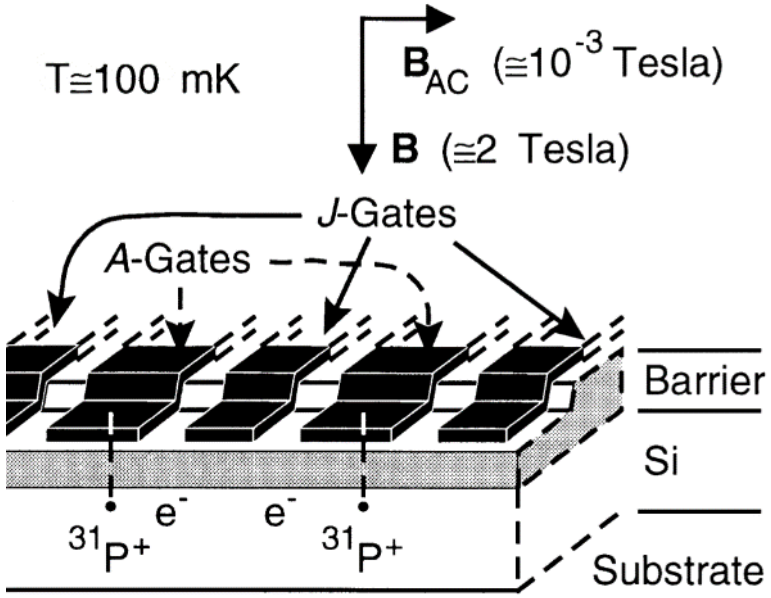

Kane, *Nature* 393, 133 (1998)

- Stoneham, Fisher, Greenland Scheme optically controlled quantum gates

- deep donor electron spin qubits
- qubit coupling controlled by orbital excited states

- **~10 - 20 nm spacing of 2 donor species**

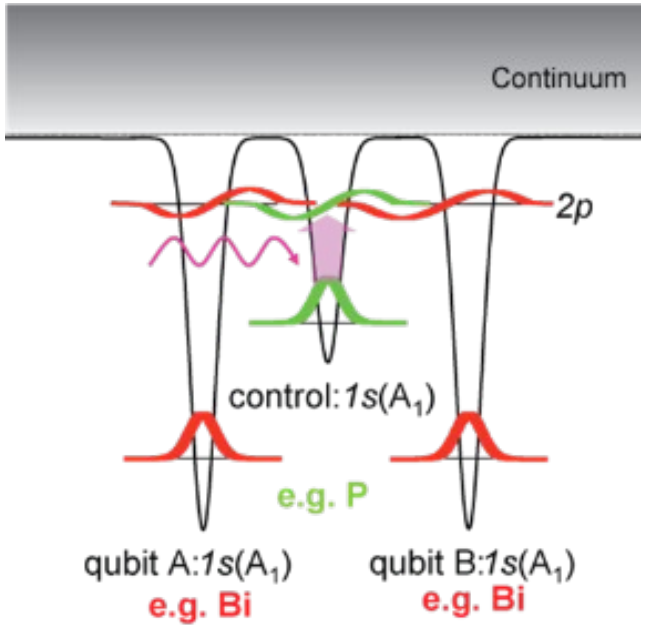

A.M. Stoneham, *et al., J. of Phys.: Cond. Matter.*, 15, L447 (2003)

Importance and potential

Quantum gates

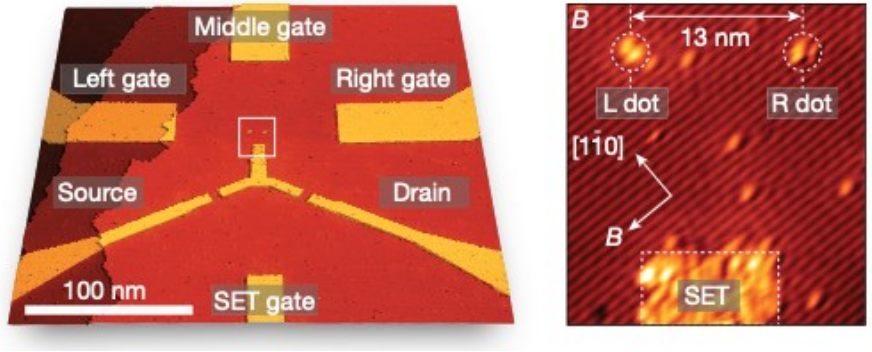

He *et al Nature* **571** 371 (2018)

Quantum simulators

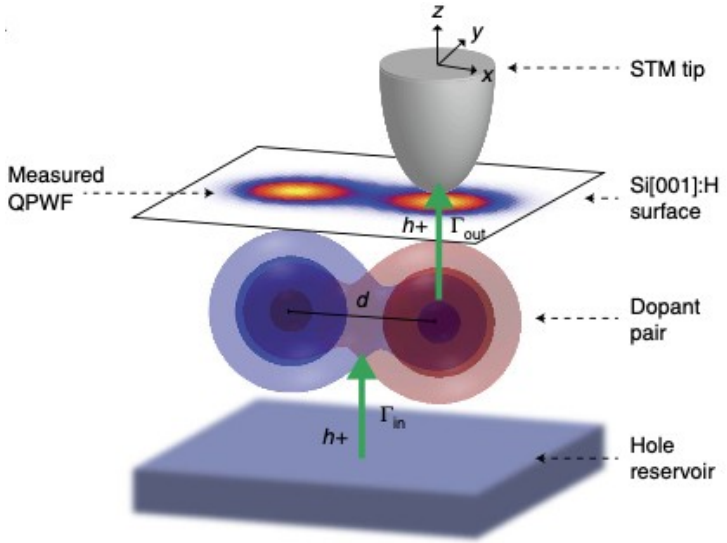

Salfi *et al Nat. Comms* **7** 11342 (2016)

New types of classical device

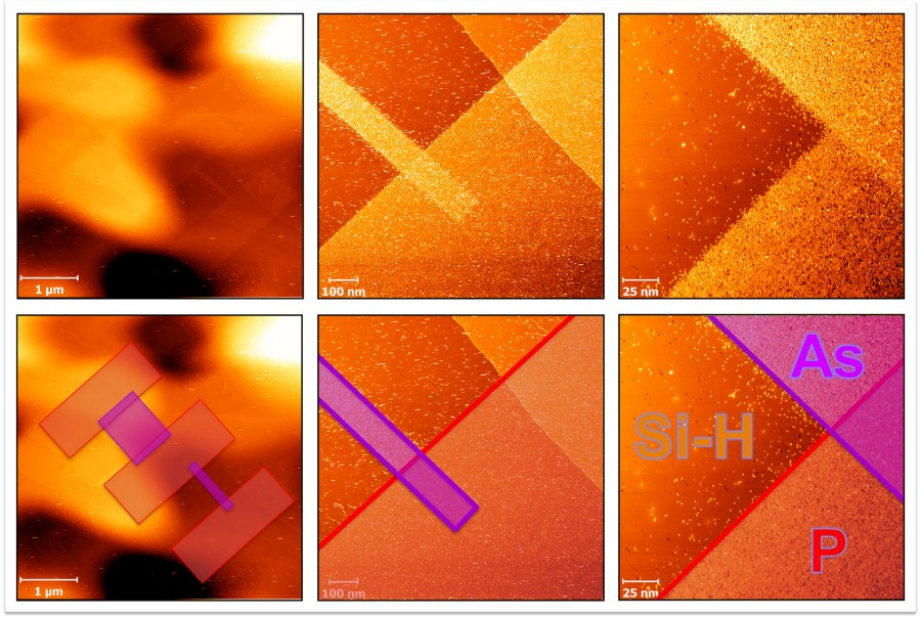

Playground for molecular and spin physics in new regimes

Thanks to: Taylor Stock, Neil Curson

Motivations and challenges for solid-state systems

- Potential advantages
  - Natural scalability (hence accessibility of thermodynamic limit)
  - Compatibility with existing semiconductor electronics (depending on materials system)
  - Access to strong interaction scales
- Likely challenges
  - Small scale of components (addressability)
  - Readout/detection
  - Maintaining coherence (hance need for cryogenics)
  - Full controllability

Example: the (Fermi-)Hubbard model

- Single-band model for hopping fermions with on-site local interactions

$$\hat{H} = -t \sum_{\langle ij \rangle} \sum_{\sigma} (\hat{c}^{\dagger}_{i\sigma} \hat{c}_{j\sigma} + \text{h.c.}) + U \sum_{i} \hat{n}_{i\uparrow} \hat{n}_{i\downarrow} \equiv \hat{H}_{\text{hop}} + \hat{H}_{\text{int}}$$

- Doping away from half-filling:

$$\sum_{i\sigma} \langle \hat{n}_{i\sigma} \rangle = N(1+\delta)$$

- Believed to describe
  - Mott metal-insulator transition
  - Possibly superconducting cuprates
  - Other strongly correlated phenomena

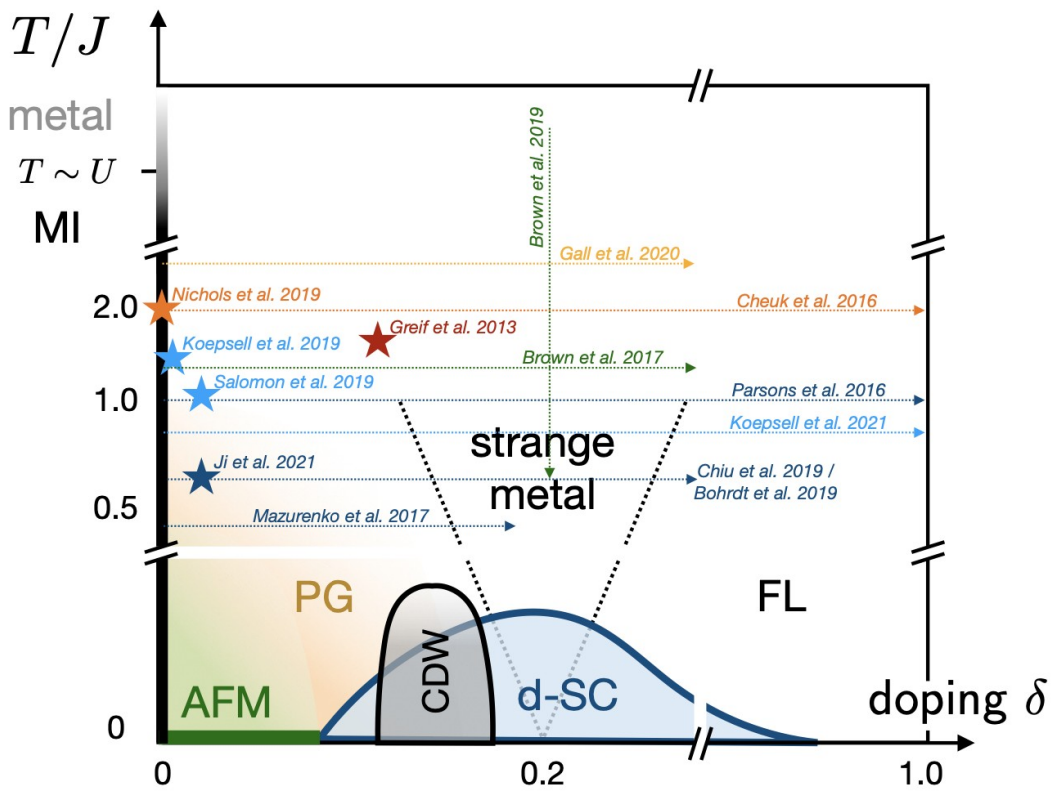

Bohrdt *et al.* arXiv:2107.08043

Effective mass theory for shallow dopants

Write perturbed potential within otherwise crystalline material as

$$V = V_0 + U$$

Expand in terms of perfect-crystal solutions as

$$\psi(\mathbf{r}) = \sum_{n\mathbf{k}} F_n(\mathbf{k})\phi_{n\mathbf{k}}(\mathbf{r})$$

where the Bloch functions satisfy

$$(\hat{T} + \hat{V}_0)|\phi_{n\mathbf{k}}\rangle = \epsilon_{n\mathbf{k}}|\phi_{n\mathbf{k}}\rangle$$

with

$$\phi_{n\mathbf{k}}(\mathbf{r}) = \mathrm{e}^{\mathbf{ik}\cdot\mathbf{r}} u_{n\mathbf{k}}(\mathbf{r})$$

Periodic function

Then the expansion coefficients satisfy

$$\epsilon_{n\mathbf{k}} F_n(\mathbf{k}) + \sum_{n'\mathbf{k}'} \langle \phi_{n\mathbf{k}}|U|\phi_{n'\mathbf{k}'}\rangle F_{n'}(\mathbf{k}') = E F_n(\mathbf{k})$$

where the potential matrix elements are

$$\langle \phi_{n\mathbf{k}}|U|\phi_{n'\mathbf{k}'}\rangle = \sum_{\mathbf{q}} \widetilde{U}(\mathbf{q}) \langle u_{n\mathbf{k}}|\mathrm{e}^{\mathbf{i}(\mathbf{q}+\mathbf{k}-\mathbf{k}')\cdot\mathbf{r})}|u_{n'\mathbf{k}'}\rangle$$

Multivalley effects for indirect-gap materials

For donors in an indirect-gap material (e.g. Si, Ge) expect dominant contributions from **k** near conduction-band minima

$$F_{n_c}(\mathbf{k}) = \sum_j \alpha_j F_j(\mathbf{k} - \mathbf{k}_j)$$

Sum goes over conduction band minima (1 for GaAs, 4 for Ge, 6 for Si)

Fourier transform to real-space envelope functions $F_j(\mathbf{r})$ for each minimum:

$$F_j(\mathbf{r}) = \sum_{\mathbf{k}} F_j(\mathbf{k} - \mathbf{k}_j) \mathrm{e}^{\mathrm{i}(\mathbf{k}-\mathbf{k}_j)\cdot\mathbf{r}}$$

These envelope functions obey

$$\int \mathrm{d}^3\mathbf{r} \sum_i \alpha_i^* F_i^*(\mathbf{r}) \left\{ [\hat{\mathbf{p}} \cdot \mathbf{A}_j \cdot \hat{\mathbf{p}} - E]\, \alpha_i F_i(\mathbf{r}) + \sum_j \alpha_j \mathrm{e}^{\mathrm{i}(\mathbf{k}_j - \mathbf{k}_i)} u^*_{\mathbf{k}i}(\mathbf{r}) u_{\mathbf{k}j}(\mathbf{r}) U(\mathbf{r}) F_j(\mathbf{r}) \right\} = 0$$

With inverse effective mass tensor

$$(\mathbf{A}_j)_{\alpha\beta} = \frac{1}{\hbar^2} \frac{\partial^2 \epsilon(\mathbf{k})}{\partial k_\alpha \partial k_\beta}\bigg|_{\mathbf{k}=\mathbf{k}_j}$$

Different valleys coupled by inter-valley matrix elements of potential (dominated by rapid variations in $U(\mathbf{r})$ and hence long-range contributions to)

Note spin-orbit effects very weak in conduction band, since c.b. consists mainly of s–states in tetrahedral semiconductors

Shindo and Nara *J Phys Soc Jpn* **40** 640 (1976)

Advantages and challenges for simulators

- Cold atoms
  - Allow easy control of hopping
  - Can reach only temperatures of the order of the hopping
  - Transport measurements challenging
  - Doping determined when trap loaded
- Semiconductor defects
  - Allow (relatively) easy control of doping via electrostatic gates
  - Able to reach low temperatures
  - Transport measurements possible
  - Parameters fixed by fabrication of device

Donors: effective mass theory for the extra electron $\Psi(\mathbf{r}) = \sum_{\mu} F_{\mu}(\mathbf{r}) u(\mathbf{k}_{\mu}) \exp(i\mathbf{k}_{\mu} \cdot \mathbf{r})$

Conduction-band minima

'Envelope function'

$$\left[-\frac{1}{2}\nabla^2 + \frac{1-\gamma}{2}\frac{\partial^2}{\partial z^2} - \frac{1}{r}\right] F_{\pm z} = \epsilon F_{\pm z} \qquad \gamma = \frac{m_{\perp}}{m_{\parallel}}$$

Scaled hydrogen atom solutions: for silicon donors

Length

Energy

} Assuming screened electric field

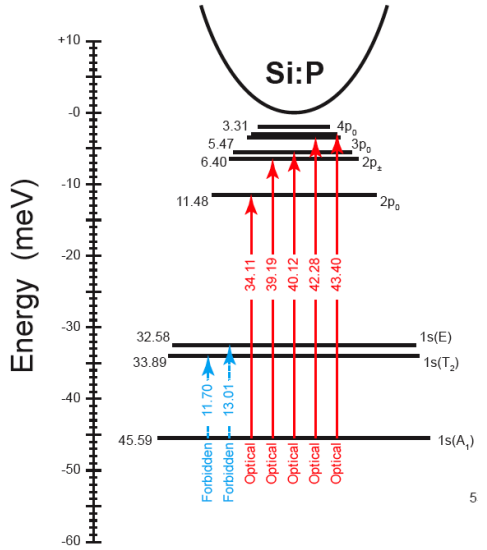

Hydrogenic orbital physics from excited states

Hubbard-like physics from lowest 1s states (splitting from intervalley coupling)

STM Lithography for Atomic Precision Doping

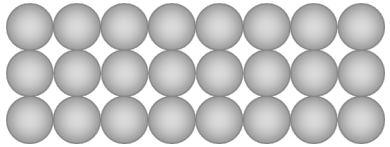

Atomically Clean Si(001)

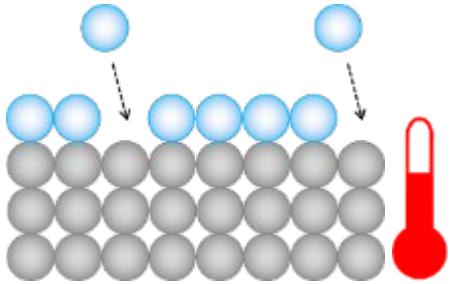

H Termination
('resist')

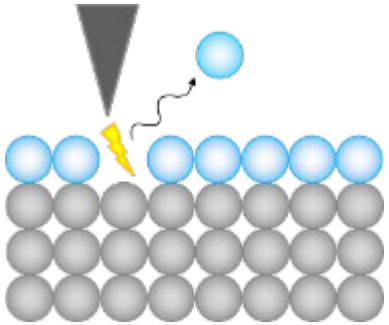

STM Lithography

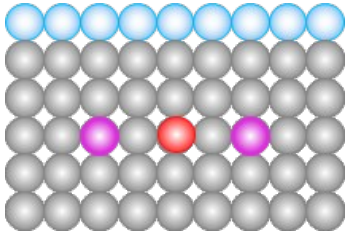

different donors
different: atomic radii,
nuclear spins,
orbital excited states

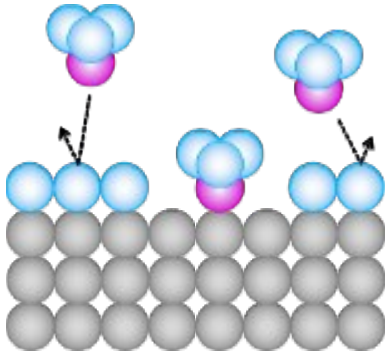

Gas Exposure
(Mol. Dissociation)

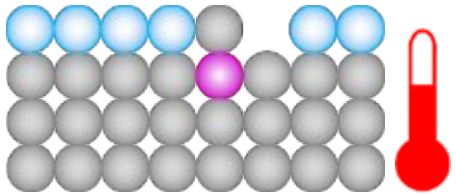

Dopant Incorporation
(Mol. Dissociation)

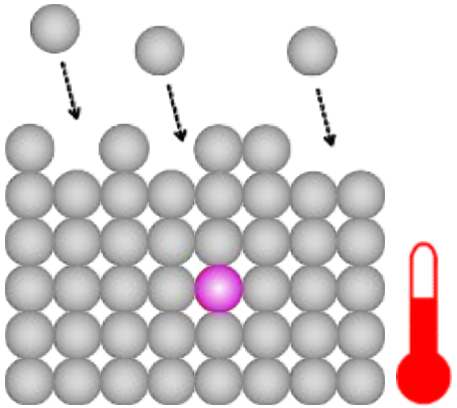

Si Encapsulation

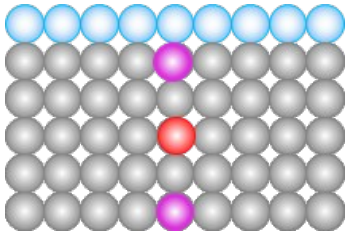

Process developed at UNSW - CQC2T

Simmons, *et al*, *Molecular Simulation*, **31** 505-515 (2006)
Stock *et al.*, *ACS Nano* **14** 3316-3327 (2020)

Silicon
Hydrogen

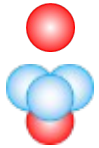

Phosphorus
Phosphine PH_3

Arsenic
Arsine AsH_3

Thanks to: Taylor Stock, Neil Curson

PH_3 Dissociation & Incorporation on Si(001)

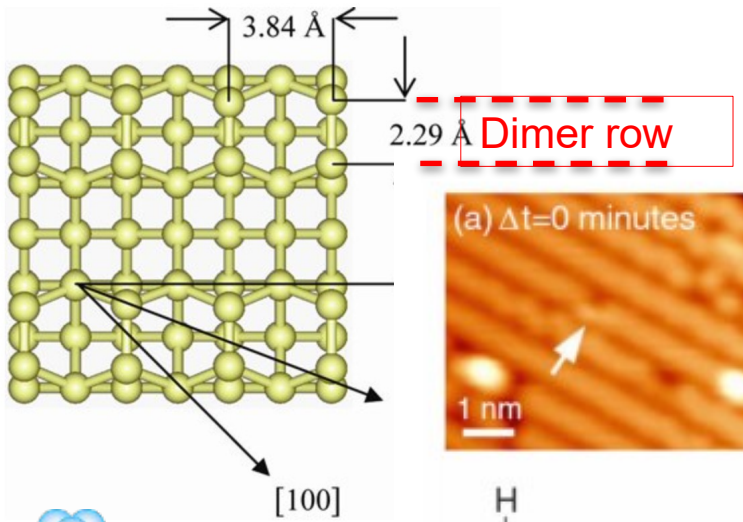

Wilson, et al, *PRB* 74, 195310 2006

Analogous structures for AsH3 calculated to be thermodynamically preferred

McDonell, et al, *Phys. Rev. B, 72* (19), 193307 (2005)

Can large arrays be created using phospine?

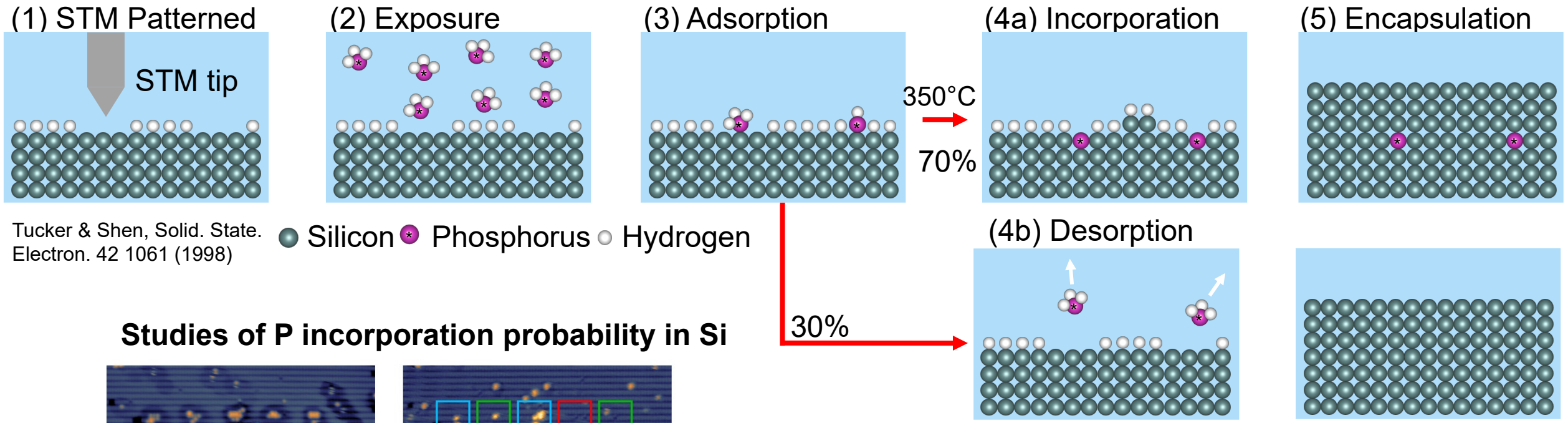

Tucker & Shen, Solid. State. Electron. 42 1061 (1998)

Studies of P incorporation probability in Si

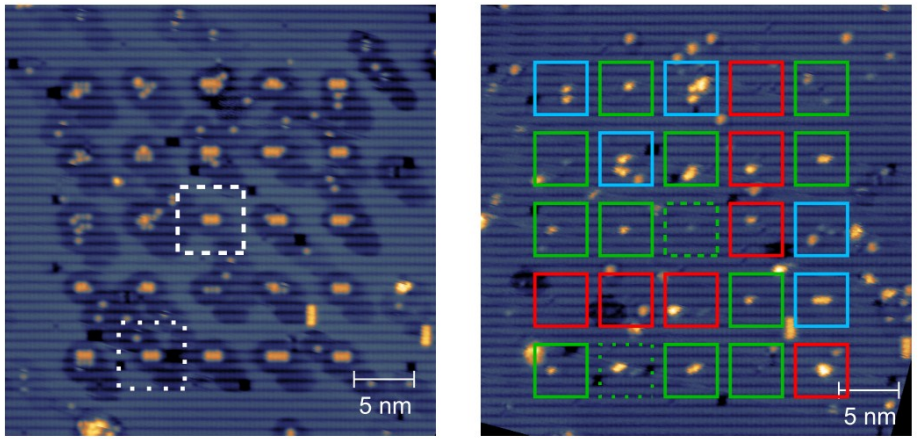

Ivie et al., Phys. Rev. Appl. 16, 054037 (2021) – Sandia group
Martin Füchsle PhD Thesis (UNSW, 2011) – UNSW group

Problem for scale-up to large number of qubits!

- Probability for fabricating qubit device:
- 50 qubit fabrication probability: 1 in 100 million.

Hydrogenic states in semiconductors: As in Si

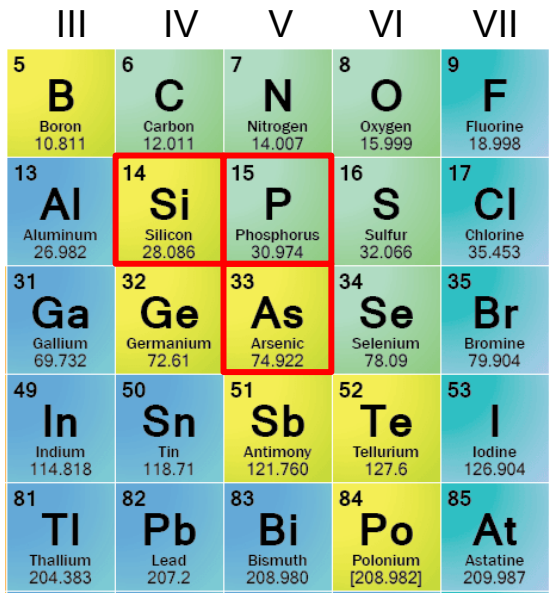

Advantages of As over P:

- Lower diffusivity.
- Larger ionisation energy.
- Spin 3/2

Disadvantages

- Smaller Bohr radii

Properties of donors in silicon

Donor	1s(A_1) (meV)	Nuclear spin	Bohr radius (nm)	Atomic radius (Å)
P	–46	1/2	1.1	1.0
As	–54	3/2	0.8	1.15

(Si 1.1 Å)

Slater, J. Chem. Phys. 41, 3199 (1964)

Larger nuclear spin

- Protocols mapping electron to nuclear spins must be implemented differently

AsH_3 Molecule Dissociation on Si(001)

PH_3 Wilson, *PRB* 74, 195310 2006

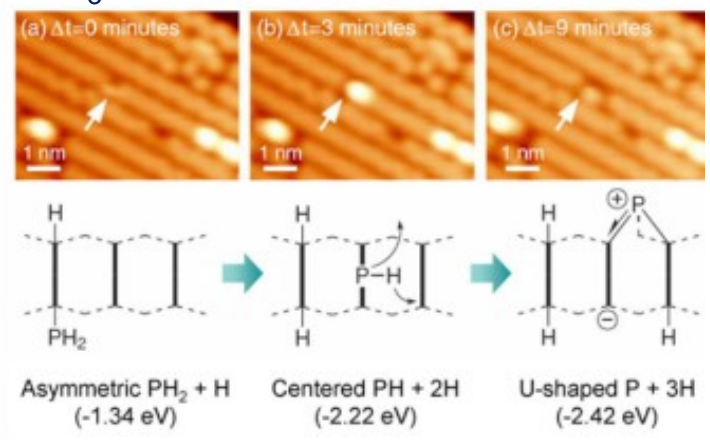

AsH_3

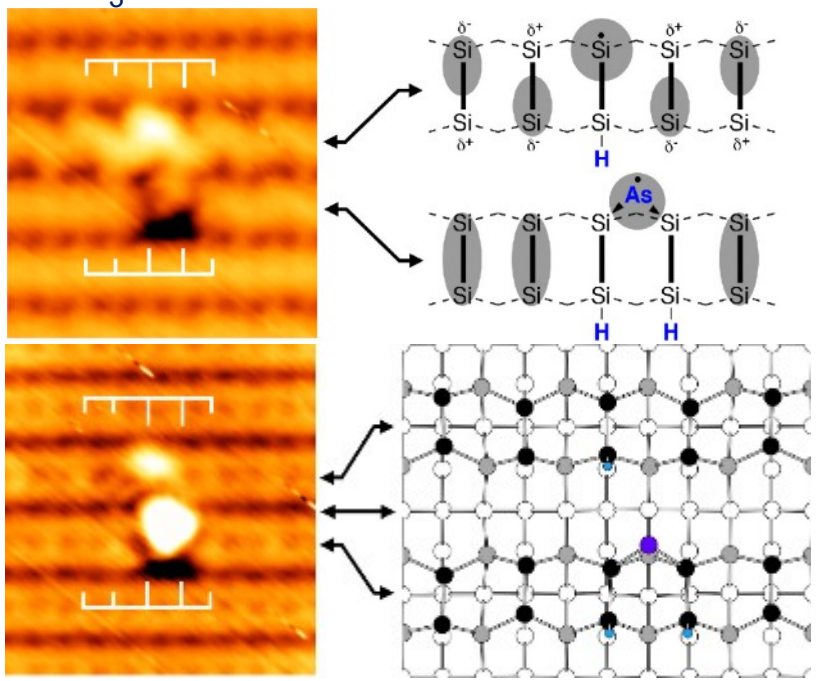

Immediate dissociation at landing site

- Isolated AsH_3 desorbs across 2 dimer rows
- *inter-row end-bridge* structure
- Alternate desorption structure is kinetically preferred for AsH_3 (As less diffusive than P)
- AsH_x do not diffuse during dissociation.

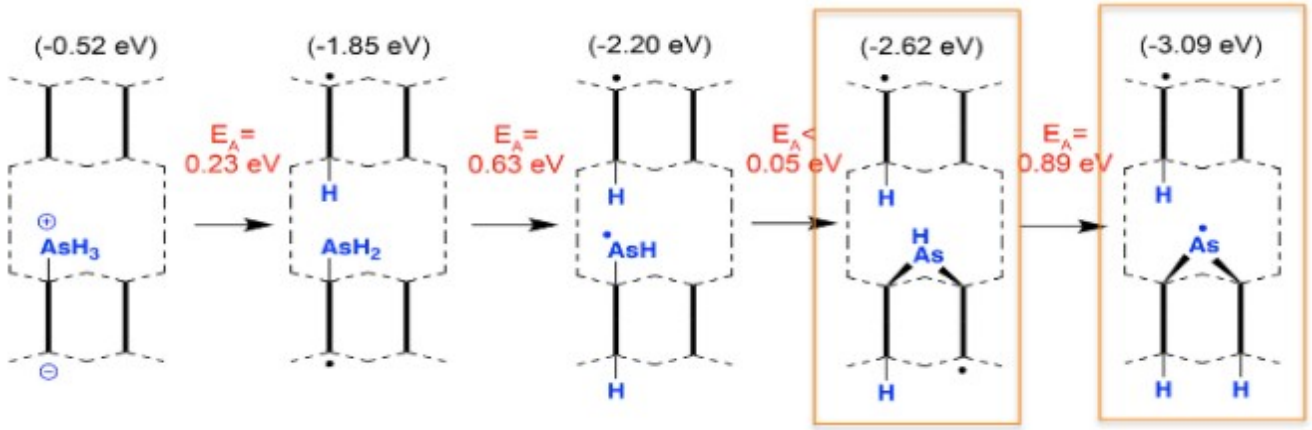

10^{-10} sec **10^{-3} sec** **10^{-1} sec**

Conclusions (Lecture 1)

- Quantum simulations may play a role in understanding otherwise intractable model Hamiltonians in the medium term
- There are computationally efficient (and practical) methods to benchmark their effectiveness, e.g. based on classical shadows and Hamiltonian learning
- Deterministic doping provides a route to controlled, well-localized quantum states within conventional semiconductor materials
- We have a well developed theoretical machinery to describe the resulting bound electronic states, based on envelope functions and effective mass theory
- Well developed for donors, possible in near term for acceptors
- Provides a natural route to analogue quantum simulations of
  - Molecular systems
  - Fermionic Mott-Hubbard models

Overview (continued)

- Lecture 2 (Wednesday)
  - Proposed (and realized) simulations with donors:
    - Molecular analogues
    - 1-d topological structures
  - ~~Quantum gates and other quantum simulation results with donors~~
  - Need for spin-orbit interactions for TIs, examples of engineered and ‘natural’ structures
  - Spherical and non-spherical models of acceptors
  - ~~Quantum Information Processing with acceptors – advantages (and disadvantages) of hole states~~
  - The honeycomb Topological Insulator
  - Detection of topological states via local probes
  - Comparison with cold-atom systems

Dopants vs quantum dots

- Individual dopants
  - Nominally identical (though environments may vary)
  - Localised states (scale set by Bohr radius) and relatively large binding energies
  - Location can be determined by implantation, properties perturbed by applied fields (electric, magnetic, strain)
  - Not otherwise controllable
- Quantum dots
  - Can produce by
    - Local clustering to relieve strain during material growth
    - Electrostatic fields from gate electrodes
  - Not identical, depend on details of fabrication
  - Typically larger regions, less localized states and smaller binding energies
  - More broadly controllable

Artificial molecules

- Isolated donor is an (electronic) analogue of the H atom
- So *N* nearby donors are an analogue of an H_N molecule
- Donors are fixed by interactions with host Si lattic so there is no nuclear dynamics
- Consequence: atoms can be frozen into far-from equilibrium arrangements inaccessible to conventional molecular physics
- Examples here: lines and 2D arrays

2-donor ‘molecules’ - experiment and theory

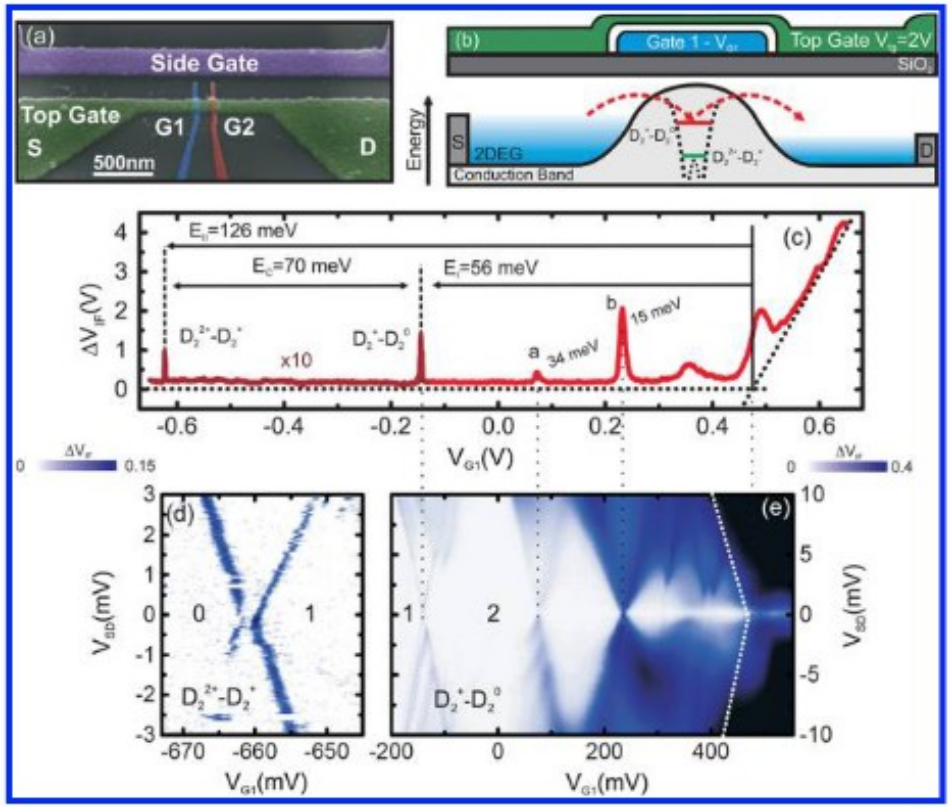

Observe charged and neutral excitations by transport measurements

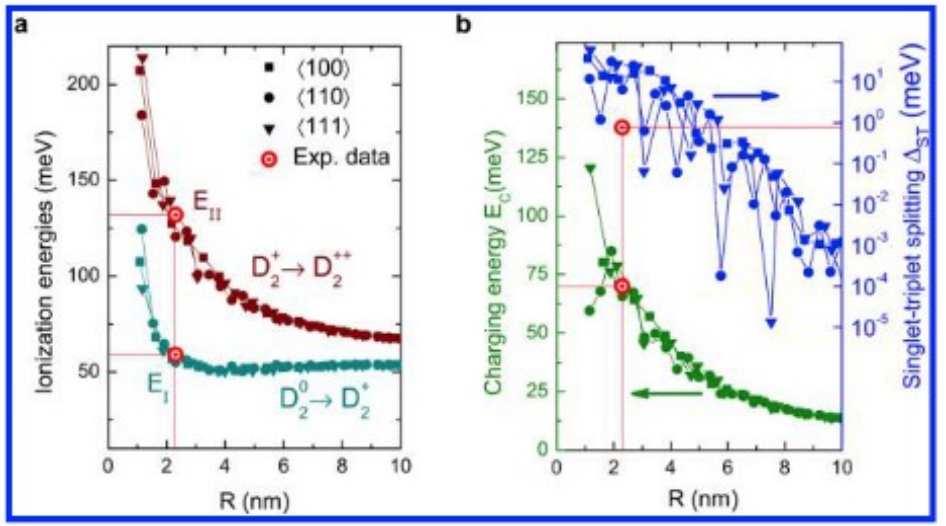

Consistent with computed excitations at 2.3nm As-As bond length

Gonzalez-Zalba, M. F. *et al*. *Nano Letters* **14**, 5672–5676 (2014).

Optical excitations of dimers and trimers

Oscillator strength as a function of frequency and geometry shows analogues of molecular transitions

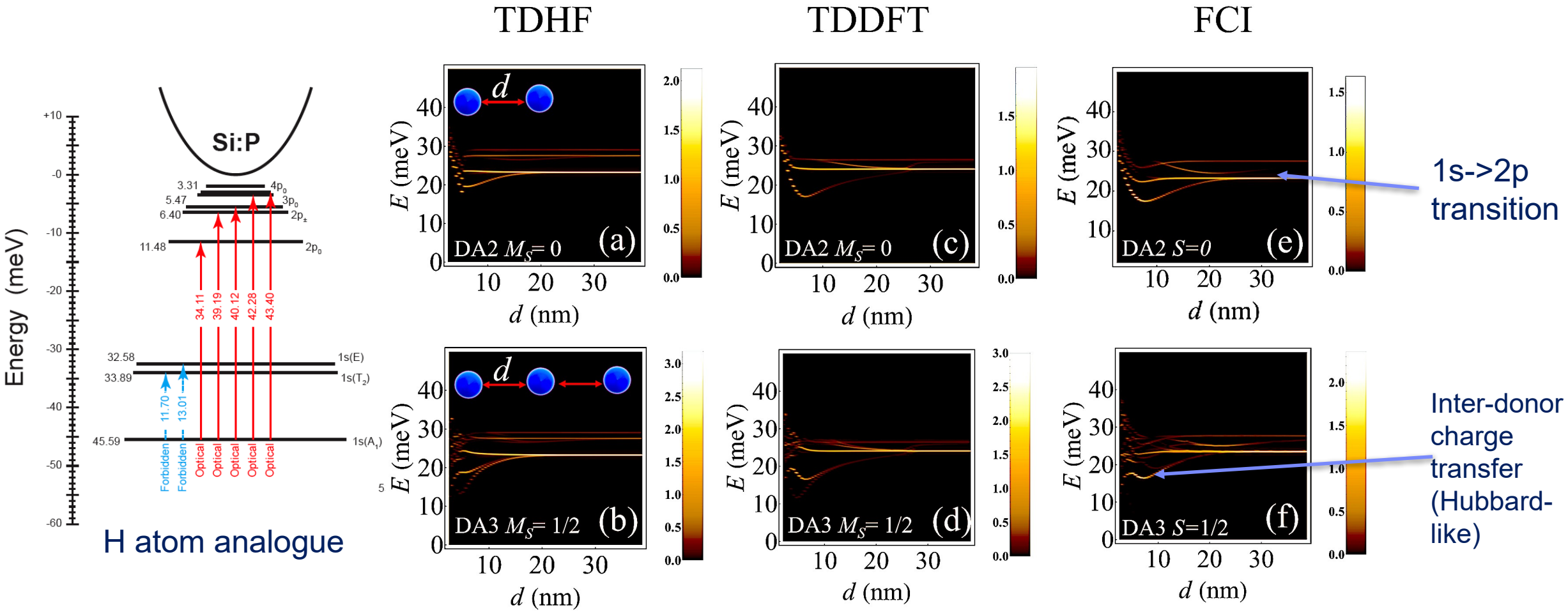

Wu *et al. Phys Rev B,* **97** 035205 (2018) doi:10.1103/PhysRevB.97.035205

Optical response of longer chains

Time-dependent density functional theory (TDDFT)

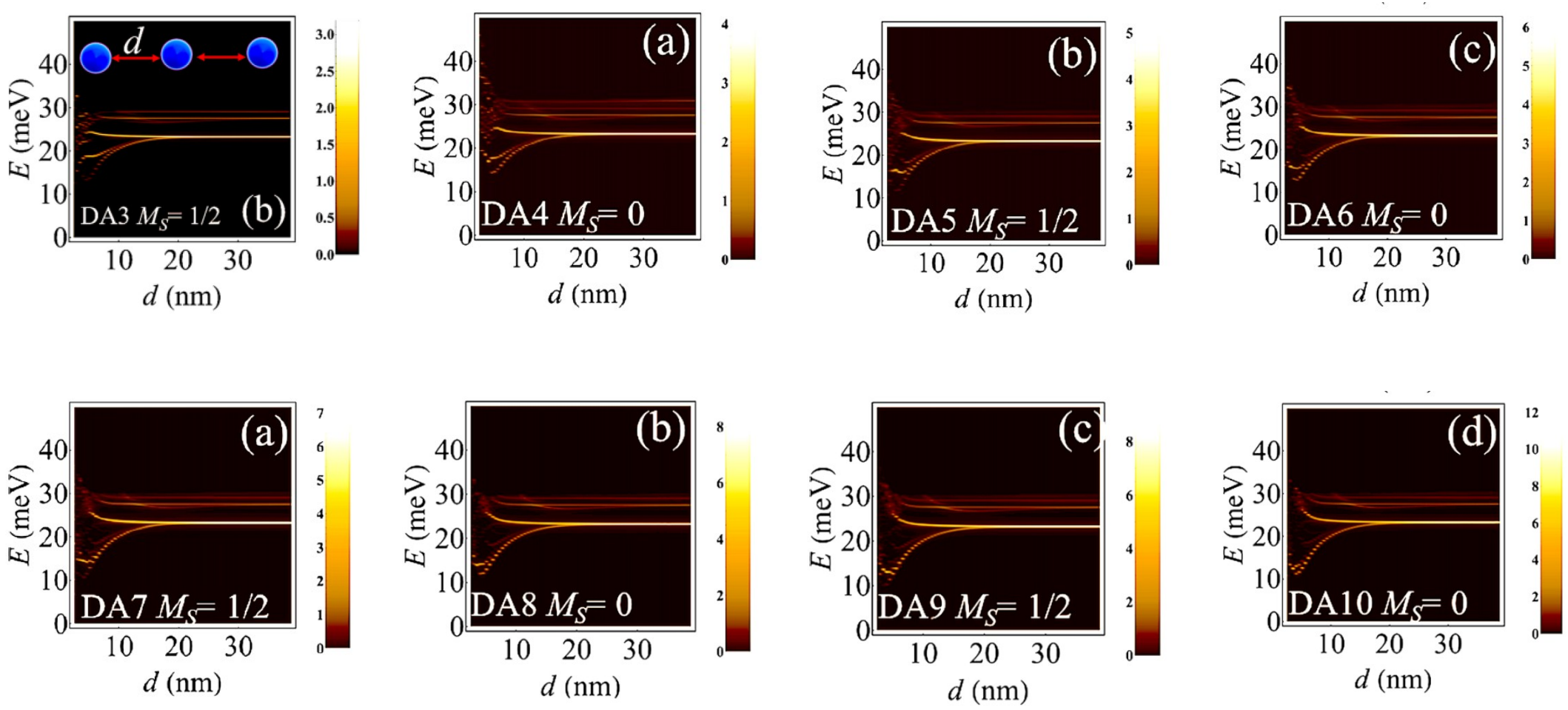

Wu *et al. Phys Rev B,* **97** 035205 (2018) doi:10.1103/PhysRevB.97.035205

Multi-valley treatment

$$\hat{H}_u = \sum_{i,A}[-\frac{1}{2}\nabla_i^2 + \frac{1-\gamma}{2}\frac{\partial^2}{\partial u_i^2} - \frac{1}{|\vec{r}_i - \vec{R}_A|}] + \sum_{i<j}\frac{1}{|\vec{r}_i - \vec{r}_j|}$$

$$\gamma = \frac{m_\perp}{m_\parallel} \quad u_i \text{ runs through } x_i,\ y_i,\ \text{and } z_i$$

$$\hat{H}_{\mathrm{mv}} = \sum_{u,w} |u\rangle[\hat{H}_u + V_{cc}]\langle u| + |u\rangle \hat{V}_{uw}^{\mathrm{VO}} \langle w|,$$

Donor dependent

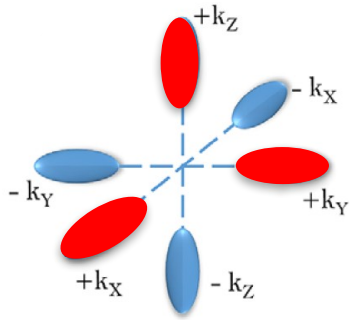

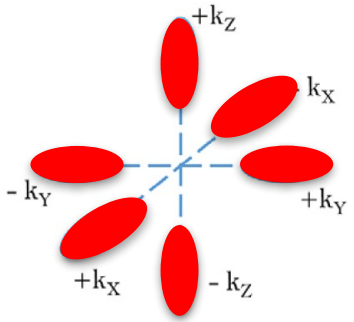

- V_{cc} is the donor-dependent central-cell correction
- Acts along [100], [110], [111] directions in terms of fcc primitive unit cell.
- Different light polarization directions along x, y, or z.
- Time-dependent Hartree-Fock methods (equivalent to RPA) implemented to compute excited states.

Wu and Fisher *Phys Rev B* **104** 035433 (2021)

Multi-valley excitation calculations for a pair

A pair of P donors along [: broken-symmetry state

Singlet state

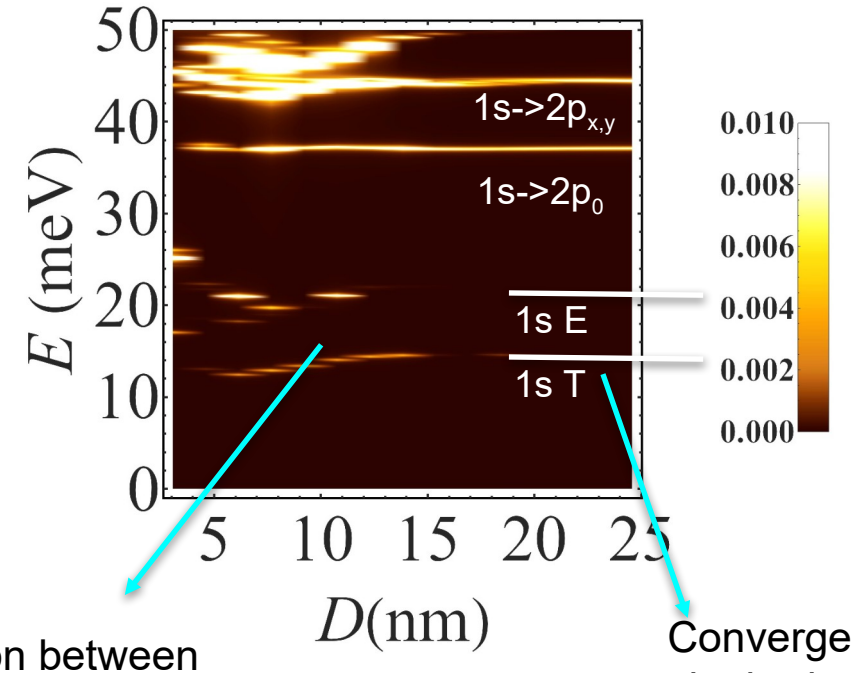

Interaction between intervalley and charge transfer

X-polarization

Converge to single-donor intervalley transitions (dark)

Triplet state

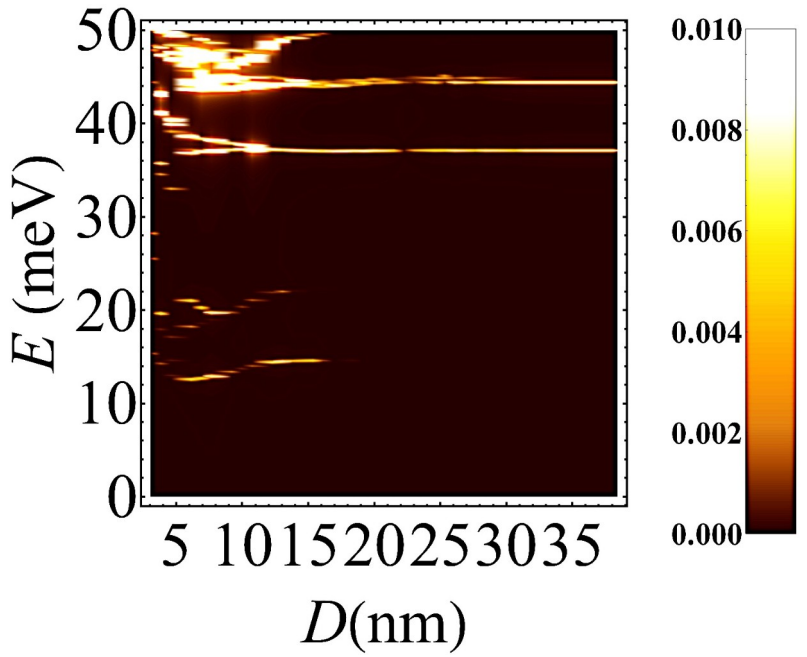

X-polarization

Comparison with experiment

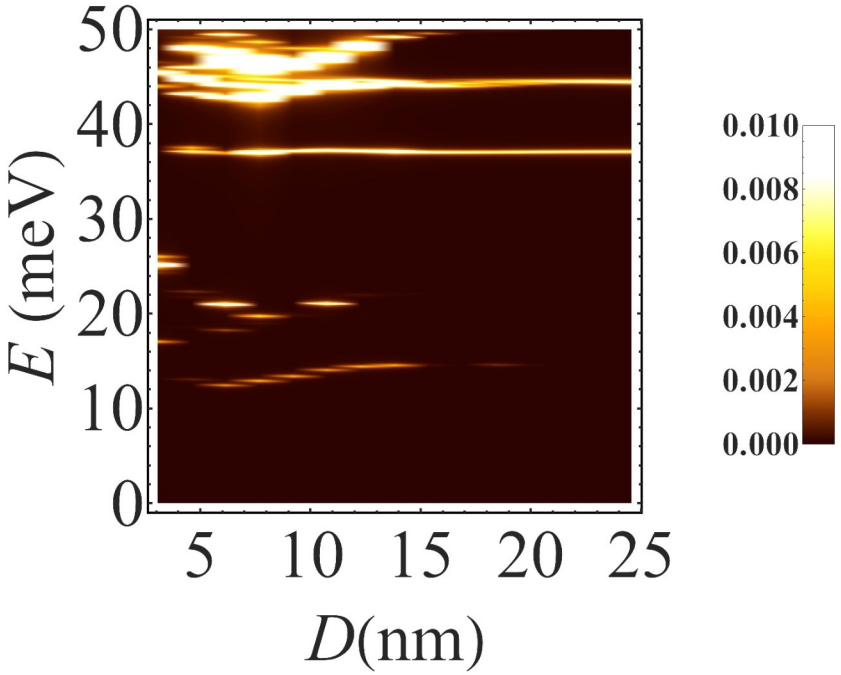

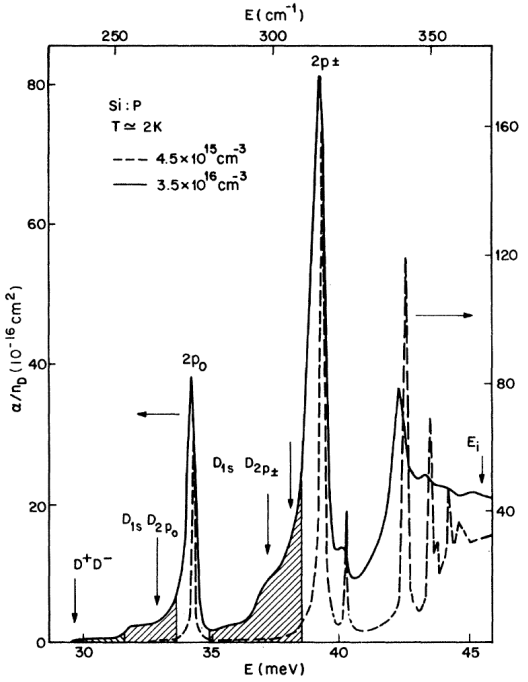

Thomas, PRB, 1981.

Feasibility study (with 'classical' theory)

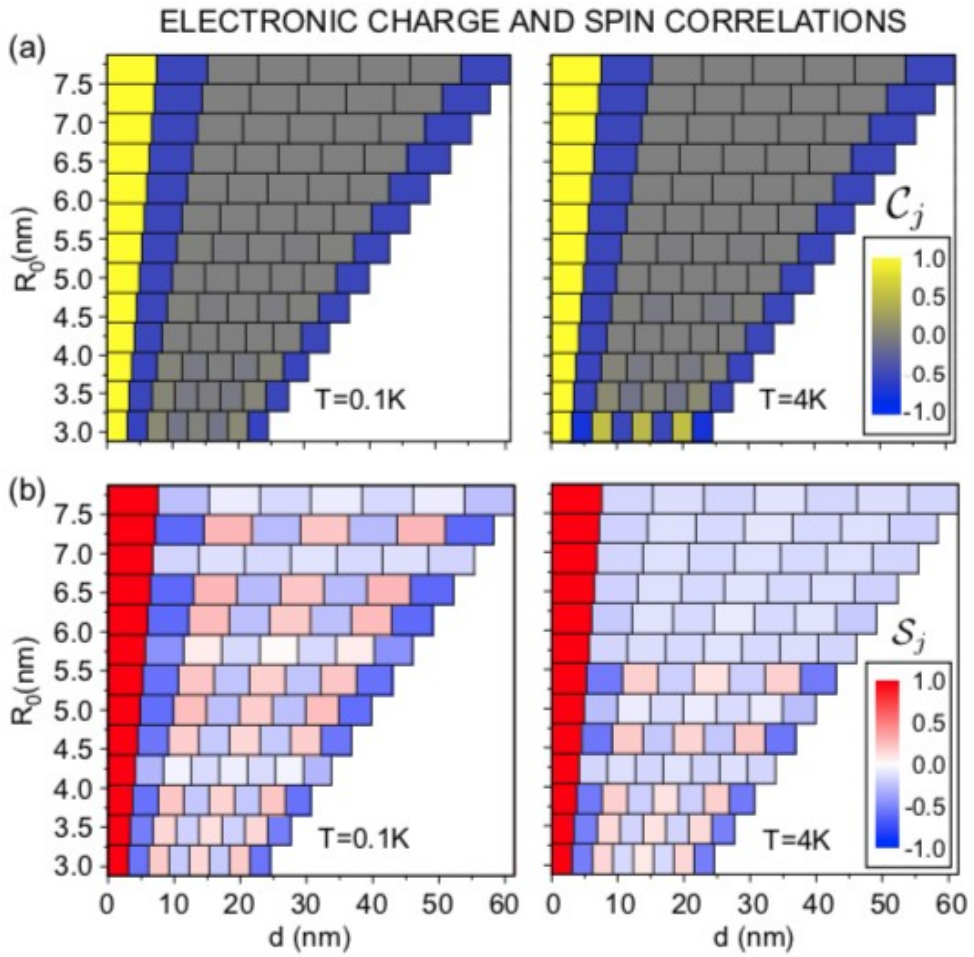

Theoretical prediction of charge and spin correlations for uniformly spaced 1D array (with periodic boundary conditions)

Dusko et al NPJ Quantum Info **4** (2018) doi:10.1038/s41534-017-0051-1

First steps (experiment)

Experimental simulation of the Hubbard model using serendipitous pairs of randomly placed acceptors, inferring tunneling processes from STM images

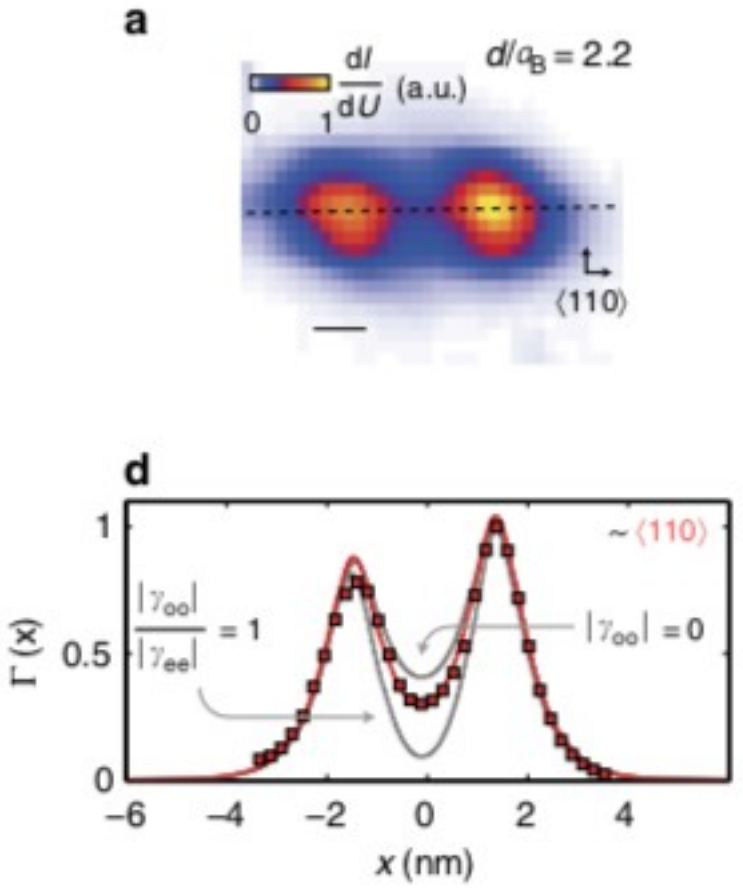

Salfi, Mol *et al.* Nature Comms. (2016) DOI: 10.1038/ncomms11342

Realizations of 2D arrays

2x2 array
(single atoms)

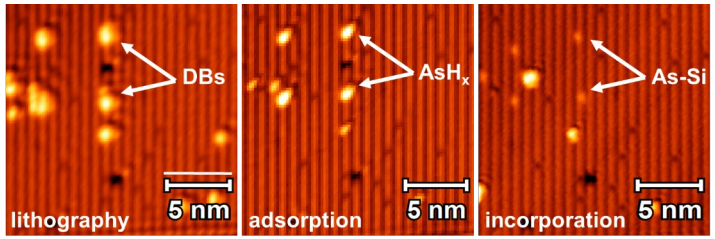

4x4 array

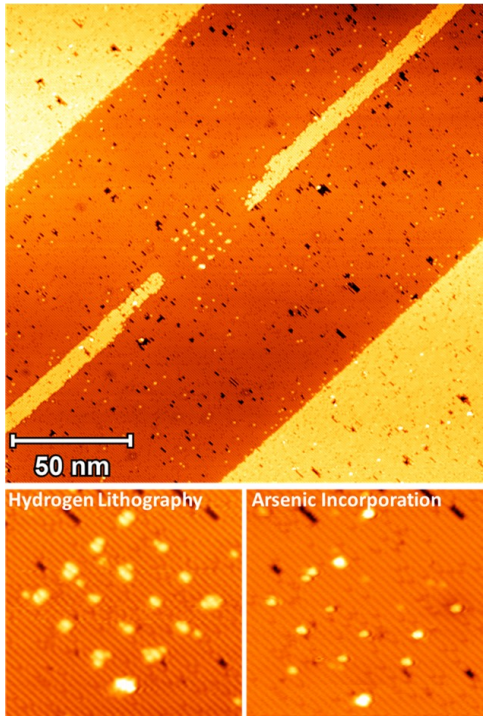

Stock et al. UCL (unpublished)

Dopant: As

3x3 arrays

Spacing:

4.1nm

6.6nm

10.7nm

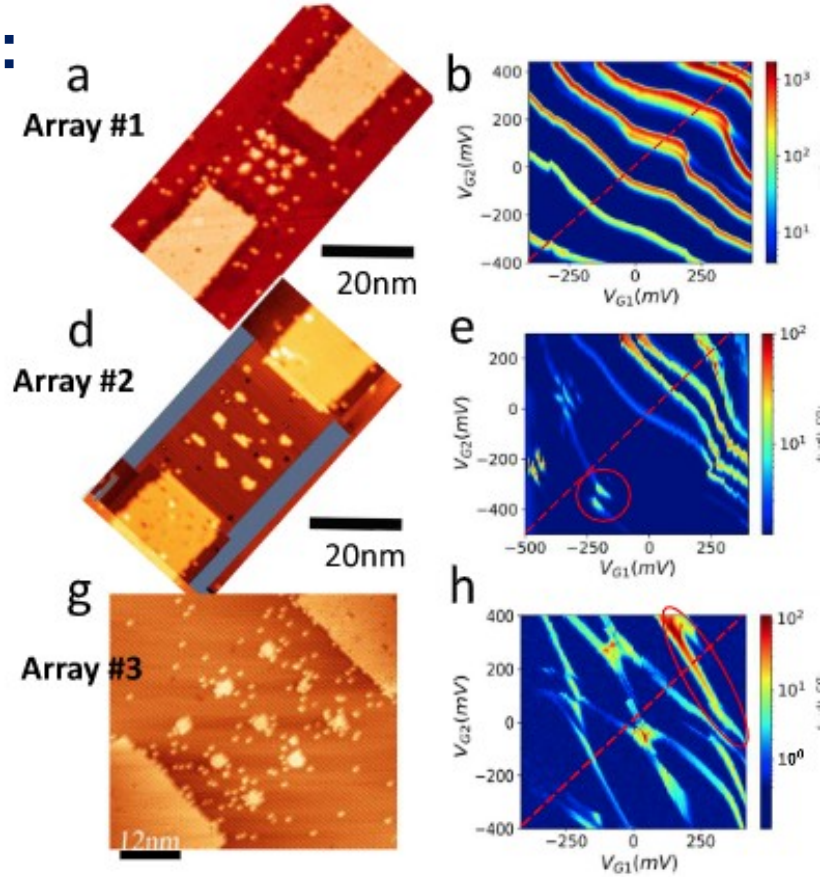

Metal

Insulator

Wang et al. (NIST group)
Nature Comms **13** 6824 (2022)

Dopant: P

Topological matter

- States characterized by their *topology* (in some space) rather than by their symmetry
- Non-interacting crystalline case: relevant electronic topology is that of the *band structure*

$$(\hat{T} + \hat{V}_0)|\phi_{n\mathbf{k}}\rangle = \epsilon_{n\mathbf{k}}|\phi_{n\mathbf{k}}\rangle$$

$$\phi_{n\mathbf{k}}(\mathbf{r}) = \mathrm{e}^{\mathbf{ik}\cdot\mathbf{r}} u_{n\mathbf{k}}(\mathbf{r})$$

- In this case the connection between the quantum states at different Bloch wavevectors **k** within the 1BZ is given by the *Berry connection*

$$\mathcal{A}_n = \mathrm{i}\langle u_n(k)|\nabla_{\mathbf{k}} u_n(k)\rangle$$

The bulk-edge correspondence

Examples where a topologically invariant bulk property has measurable consequences at the boundary of the system

Bulk invariant	Bulk interpretation	Surface property
$\phi = \mathrm{i}\int_{-\pi/a}^{\pi/a} \langle u(k)\vert \frac{\partial u(k)}{\partial k}\rangle \,\mathrm{d}k = -\frac{e}{2\pi}\int_{BZ} \mathrm{Tr}[\mathcal{A}]\,\mathrm{d}^d k$	Ferro-electric polarization	Surface charge
$\sigma_{xy} = \frac{e^2}{\hbar}\int_{BZ} \frac{\mathrm{d}^2 k}{(2\pi)^2}[\nabla \times \mathcal{A}(\mathbf{k})]$	Hall conductance	Surface current
$P_3 = -\frac{e^2}{2\pi h}\int_{BZ} \mathrm{d}^3 k\, \epsilon_{abc}\mathrm{Tr}\left[\mathcal{A}_a \partial_b \mathcal{A}_c - \frac{2\mathrm{i}}{3}\mathcal{A}_a \mathcal{A}_b \mathcal{A}_c\right]$	Magneto-electric polarization	Surface spin current

Non-interacting SSH chain

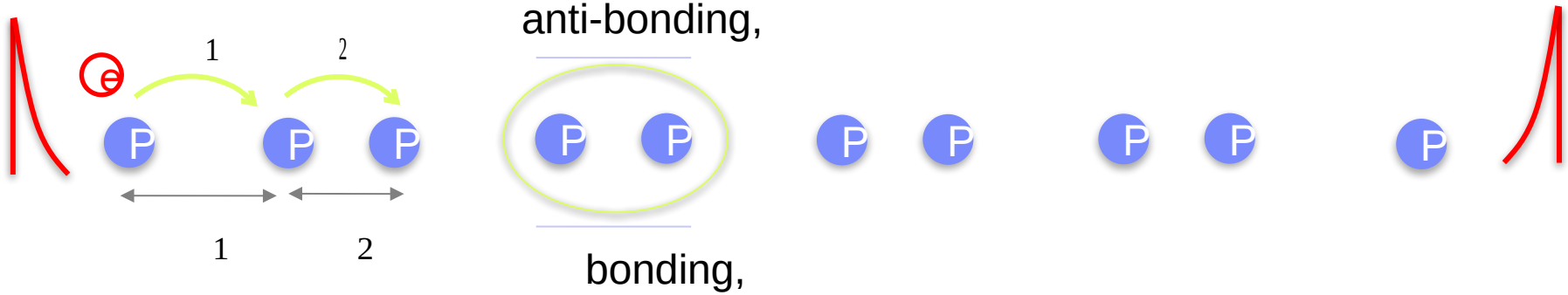

1) single-particle energy spectrum of the bulk:

2) Zak phase: a topological property of the bulk

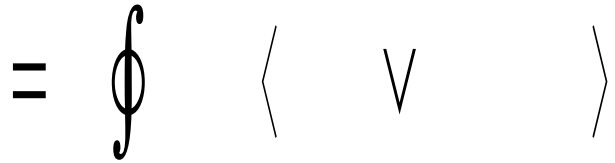

3) Topological phase transition:

- trivial phase, no edge states,
- non-trivial phase, localized edge states exist, mid-gap energy levels,

Interactions and edge states

- Beenakker's rate equations for quantum dots
- Conductance spectrum reveals the addition energy spectrum

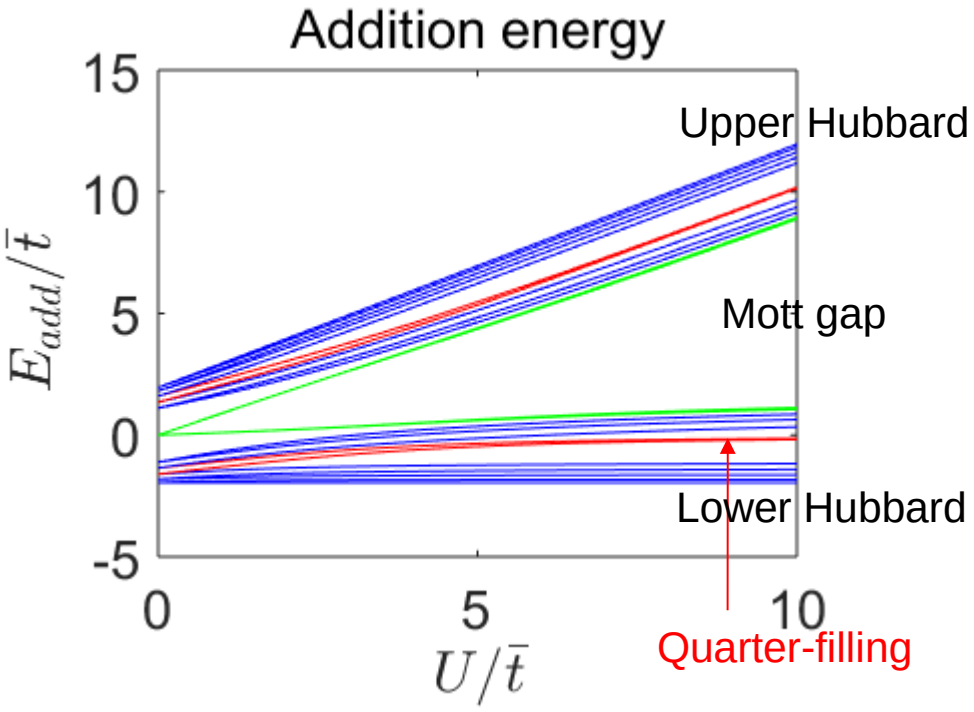

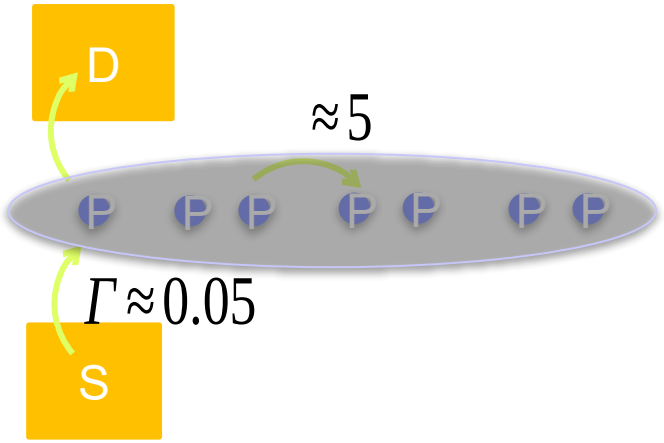

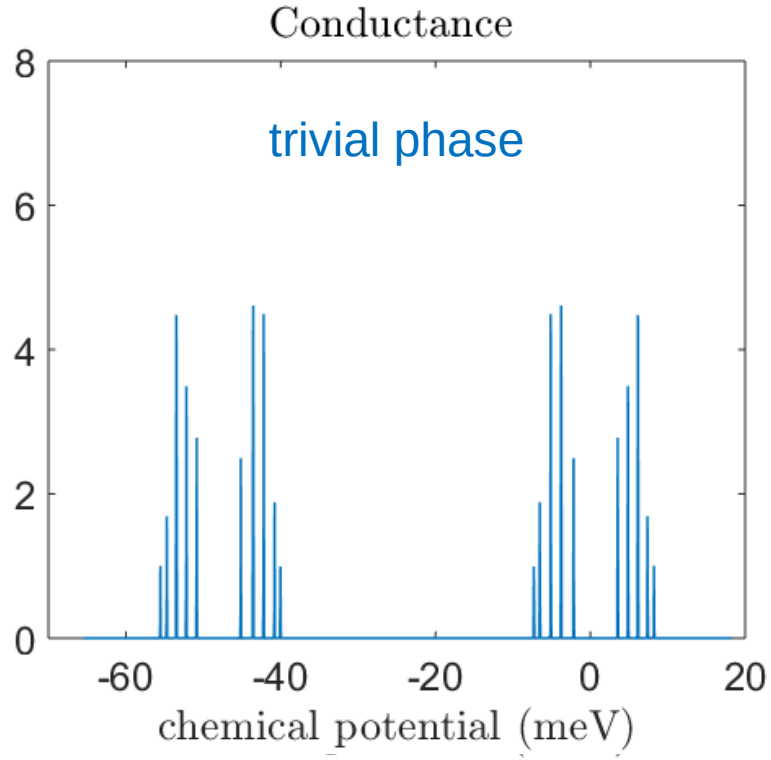

Le et al NPJ Q Info **6** 24 (2020)

Edge populations (charges)

Non-trivial phase,

: number of electrons in the chain
: number of electrons at the edges

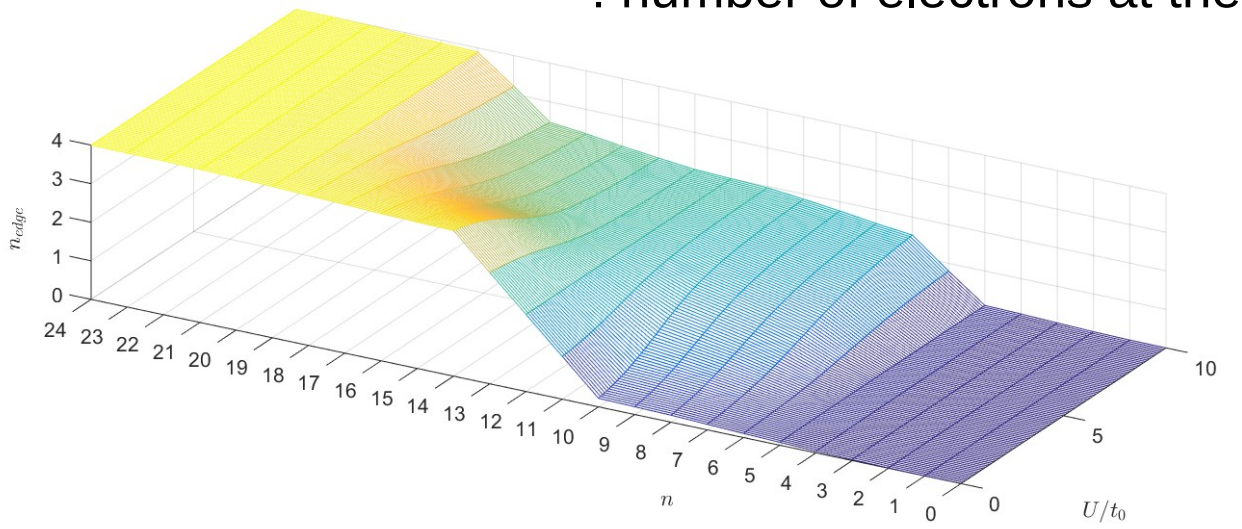

Charge-sector edge states go from half filling to quarter filling in large-U limit

$_1 = 0$ $_2 > 0$

SSH-Hubbard phase diagram (half-filling)

Add on-site interactions: Hubbard model

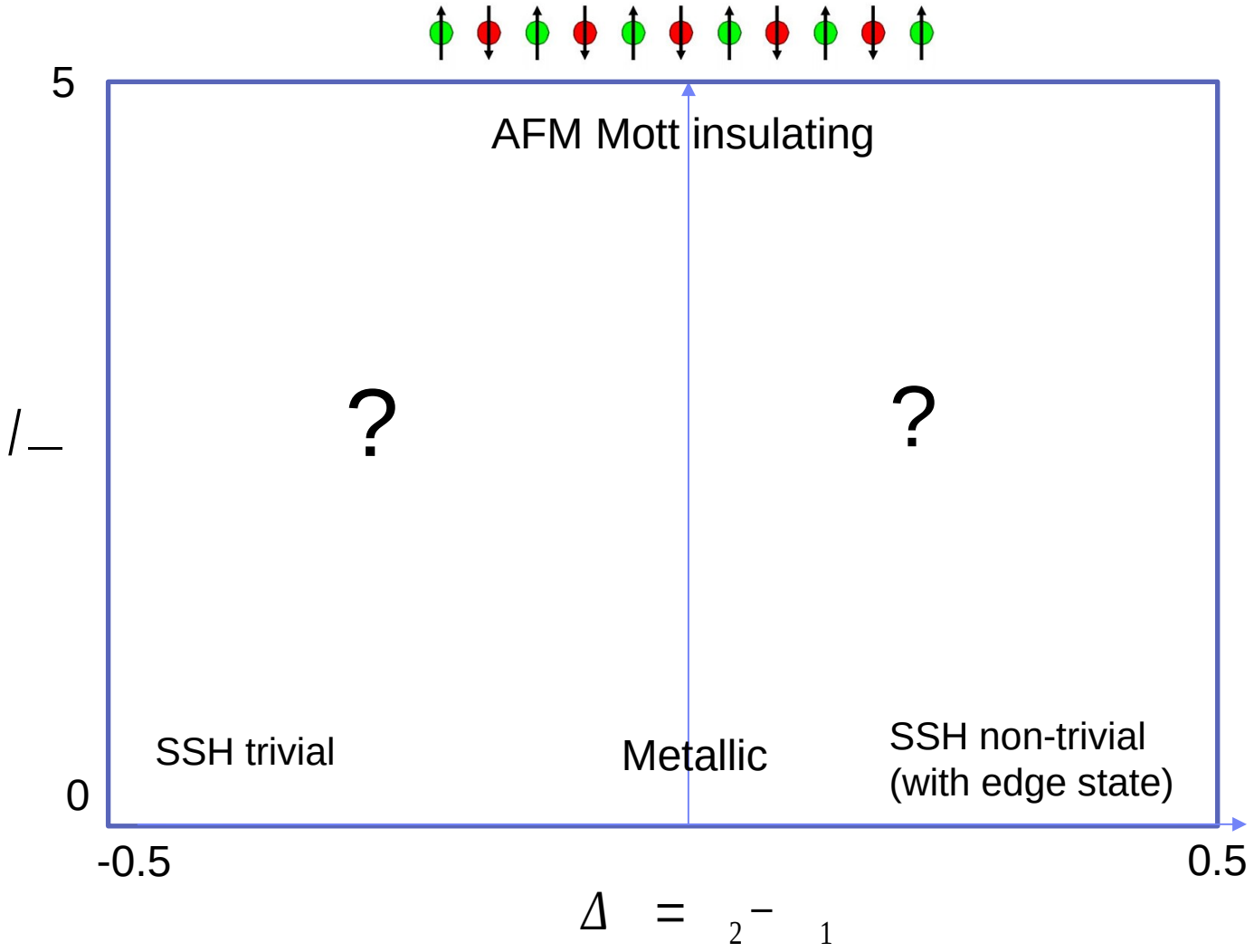

Strong interaction limit

Half-filling, Heisenberg spin chain with

Hubbard model

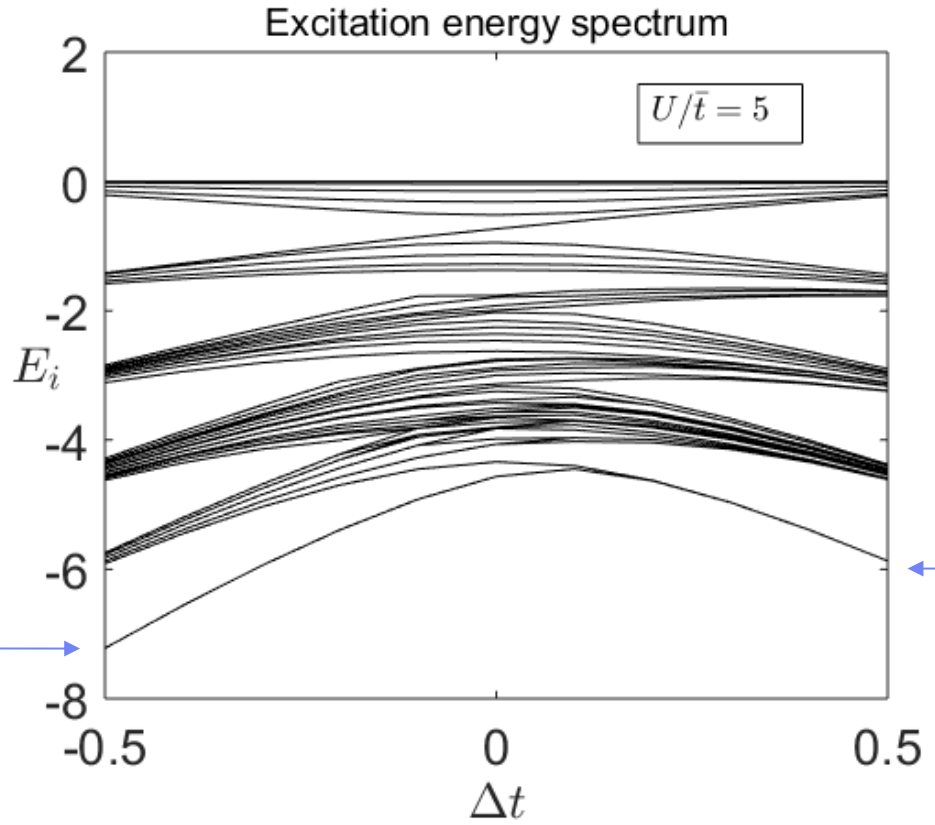

$$\mathcal{H} = \frac{1}{2}\sum_{\substack{i,j \\ i\neq j}} J_{ij}\boldsymbol{S}_i \cdot \boldsymbol{S}_j.$$

unique ground state

4 degenerate ground states

electrons form a singlet in each dimer, the spin at the edges are free

Two edges:

Bulk dimers:

Le et al NPJ Q Info **6** 24 (2020)
doi:10.1038/s41534-020-0253-9

Ground state spin correlation

non-trivial phase (), half filling,

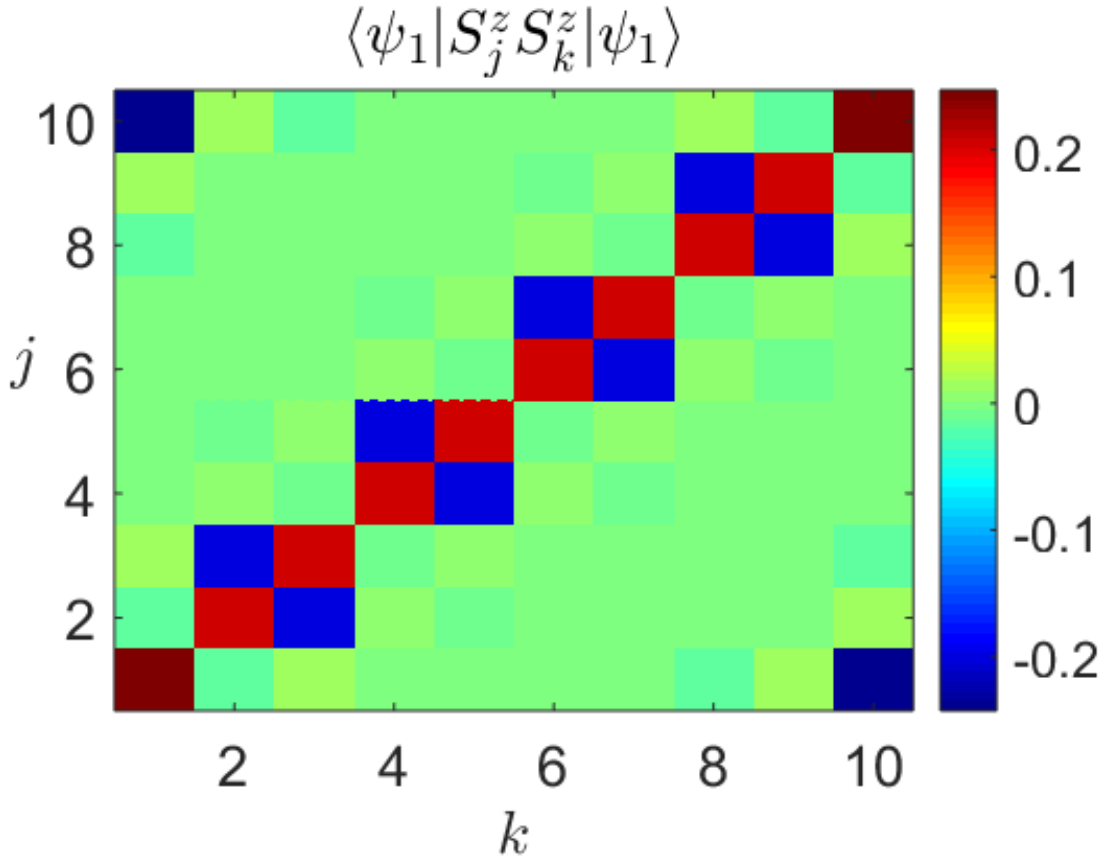

Ground state spin correlation

$\langle \hat{S}_j^z \hat{S}_k^z \rangle$

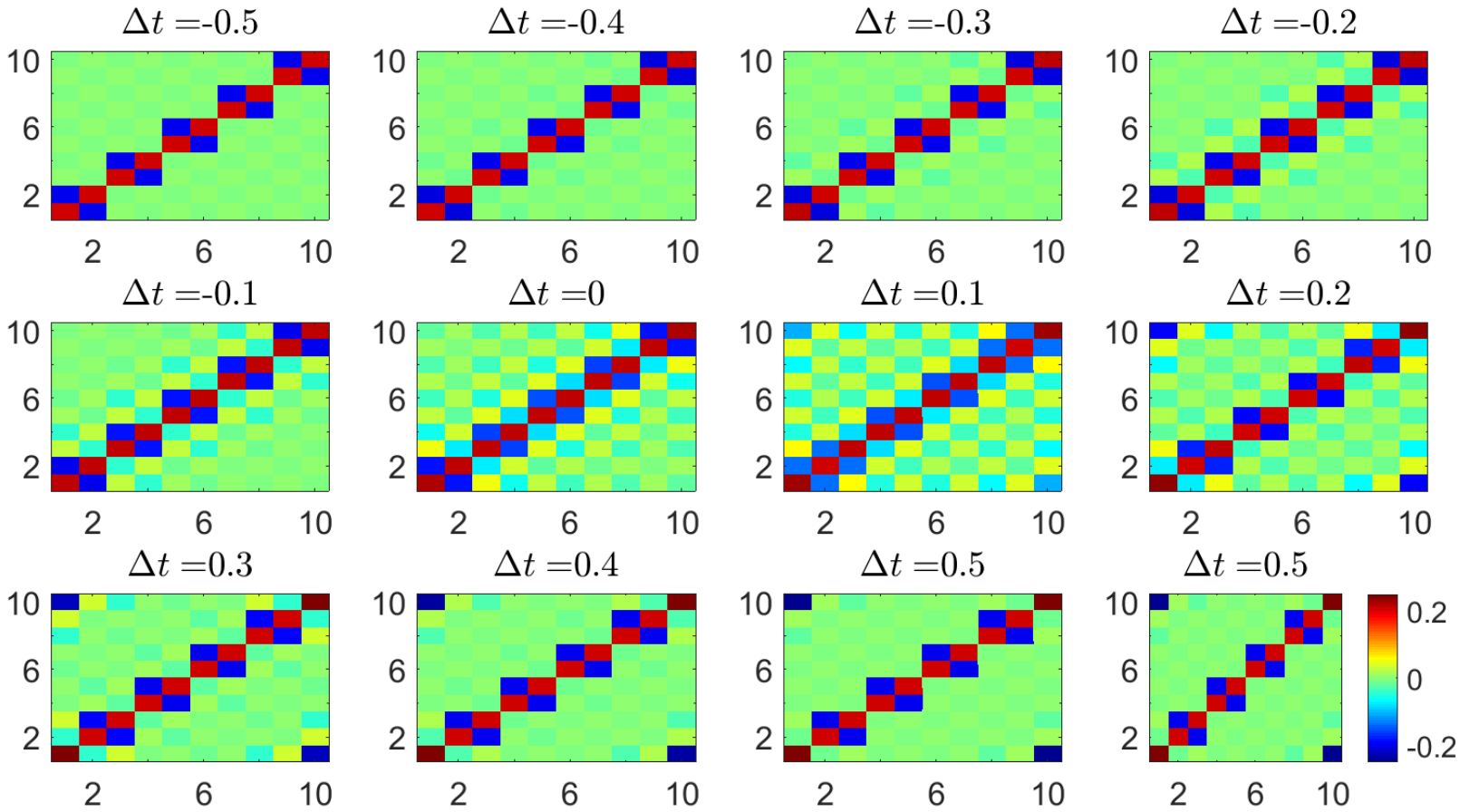

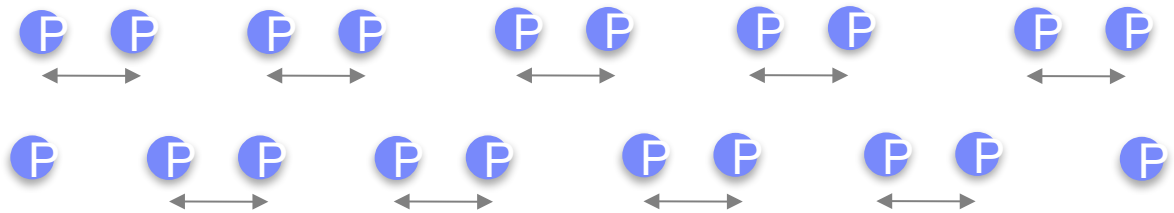

Le et al NPJ Q Info **6** 24 (2020)
doi:10.1038/s41534-020-0253-9

SSH-Hubbard phase diagram (half-filling)

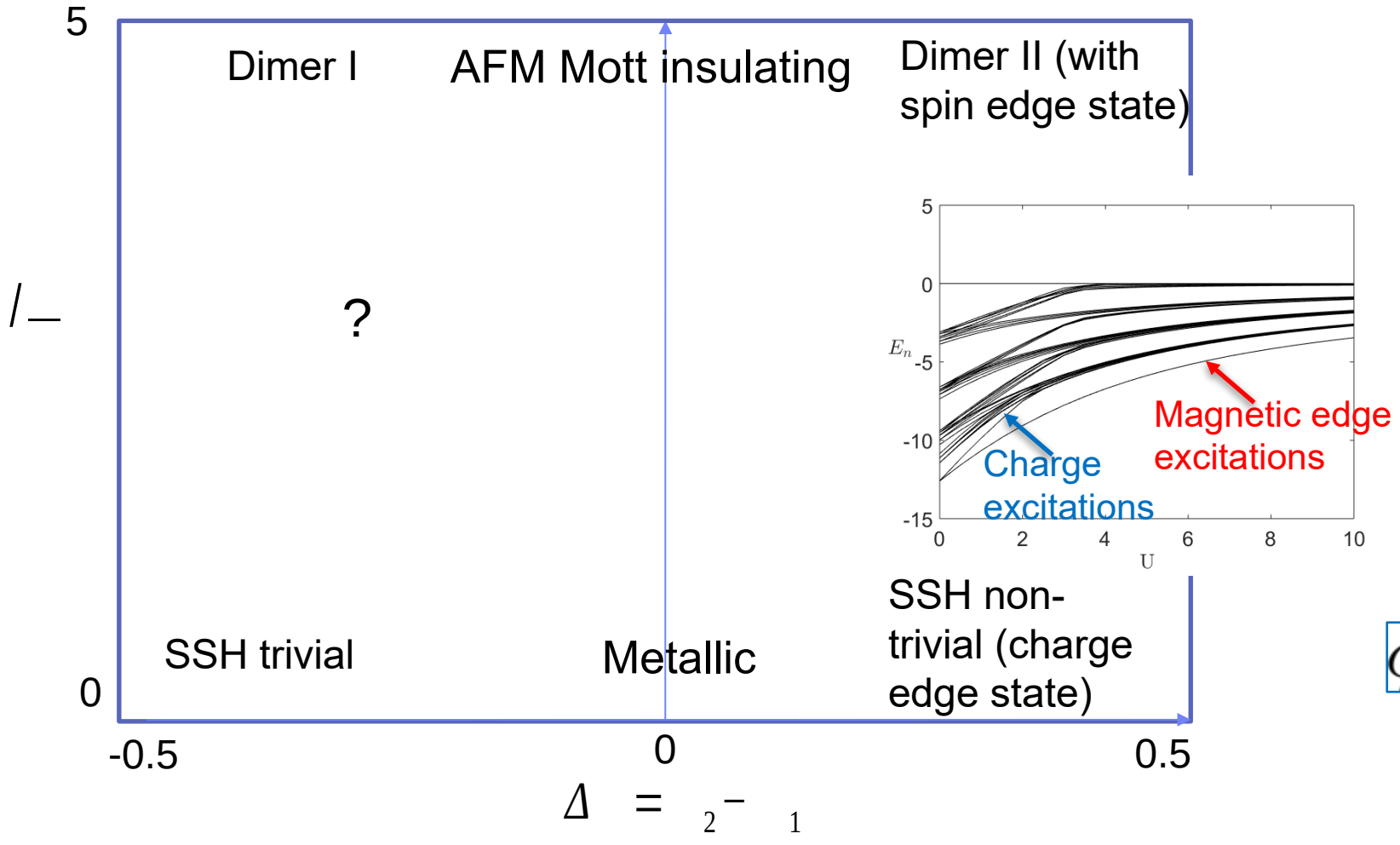

$\phi_A = 0$

$\phi_A = \pi$

Le et al NPJ Q Info **6** 24 (2020)
doi:10.1038/s41534-020-0253-9

Reduced (many-body) Zak phase $= arg(\quad) = arg\left(\quad \prod_{=1}^{-1} \quad (\quad)\right) = \quad \frac{2}{} \sum_{\in}^{\square}$ ()

Experimental realization

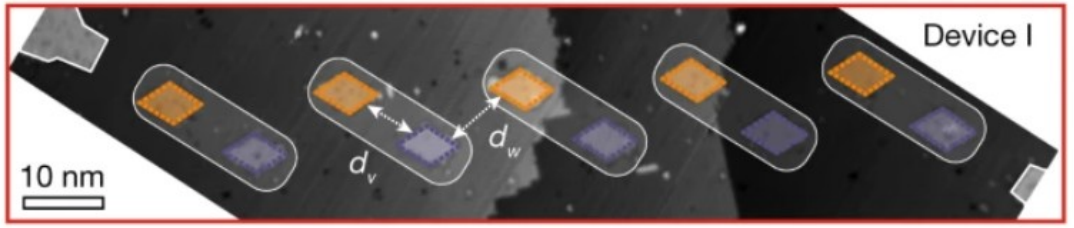

Trivial: $v > w$, $d_v < d_w$ $d_v = 7.7$ nm, $d_w = 10.1$ nm

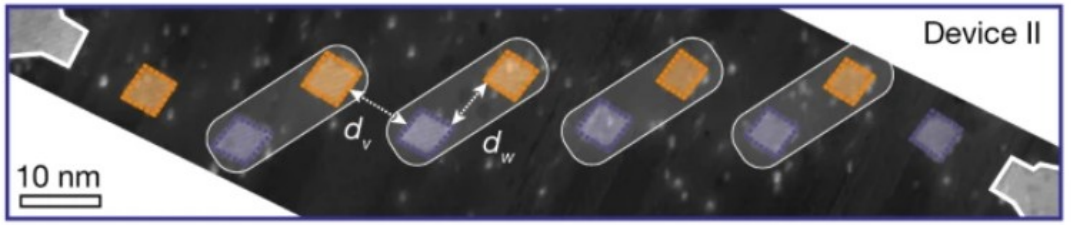

Topological: $v < w$, $d_v > d_w$ $d_v = 9.6$ nm, $d_w = 7.8$ nm

Line of deterministically implanted multi-donor quantum dots

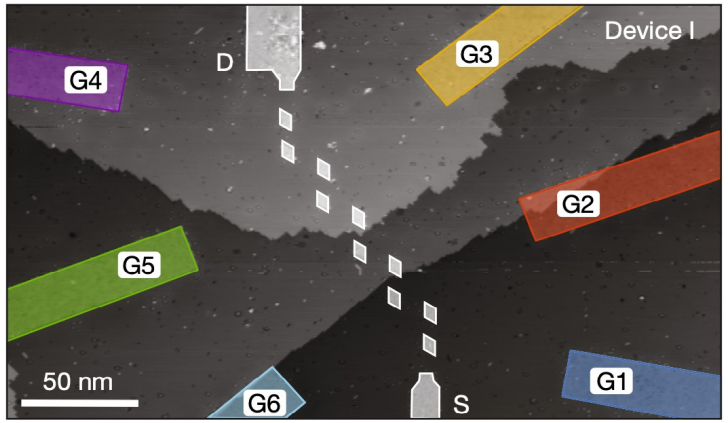

Controlling gates tuned for maximum conductance

Trivial phase: transport whenever two charge states are degenerate (Coulomb blockade)

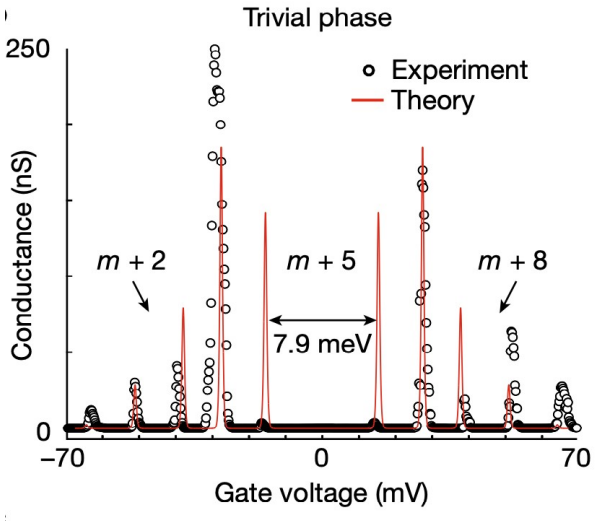

Topological phase: only edge states have weight at chain ends and can connect to source and drain

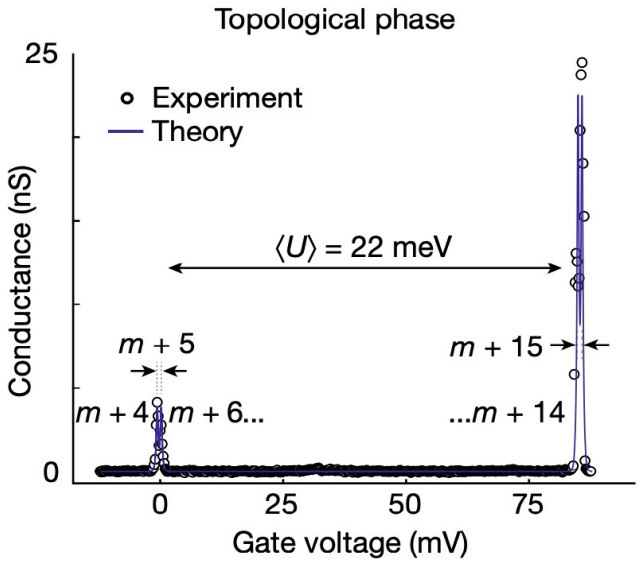

Kyczynski et al (UNSW group) *Nature* **606** 694-9 (2022)

A cold-atom approach

- Direct measurement of Zak phase with 1D lattice of bosonic atoms (^{87}Rb)

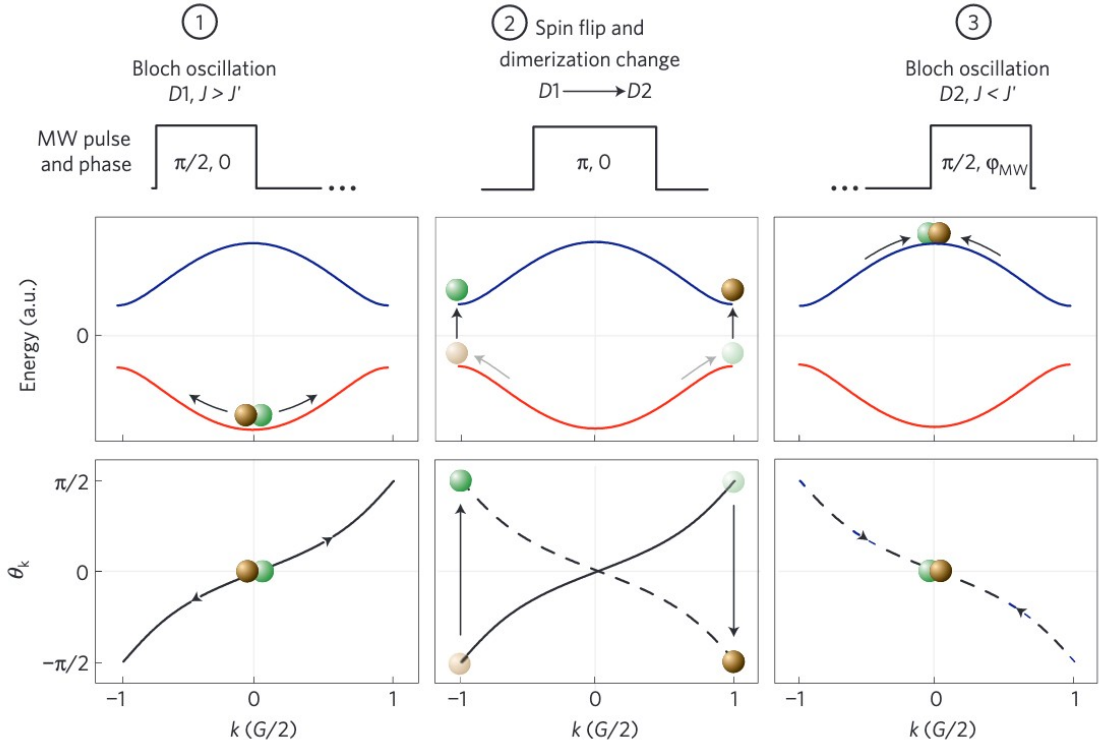

1. Prepare in

$$|\Psi(t=0)\rangle = \frac{1}{\sqrt{2}}\left(|\uparrow, k=0\rangle + |\downarrow, k=0\rangle\right)$$

using microwave pulse

2. Apply opposite forces to and with a field gradient

$$\hbar\dot{k} = \pm F_{\text{applied}}$$

$$|\Psi(t)\rangle \propto \frac{1}{\sqrt{2}}\left(|\uparrow, k\rangle + \mathrm{e}^{\mathrm{i}\delta\phi}|\downarrow, -k\rangle\right)$$

3. Invert spin (using - pulse) and change sense of dimerization, swapping lower and upper bands

4. Evolve back to k=0 (cancelling phase differences from Zeeman effect) and measure final phase difference

$$\delta\phi = \phi^{D1}_{\text{Zak}} - \phi^{D2}_{\text{Zak}}$$

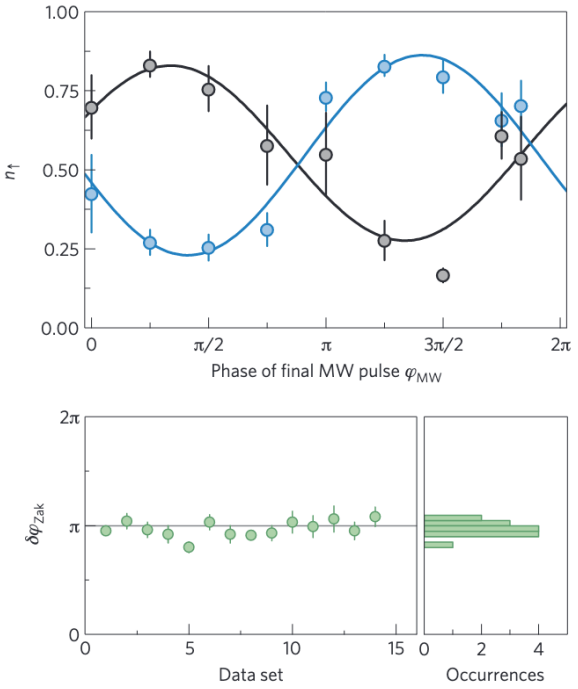

Atala *et al. Nat. Phys.* **9** 795 (2013)

Donors and cold atoms - comparison

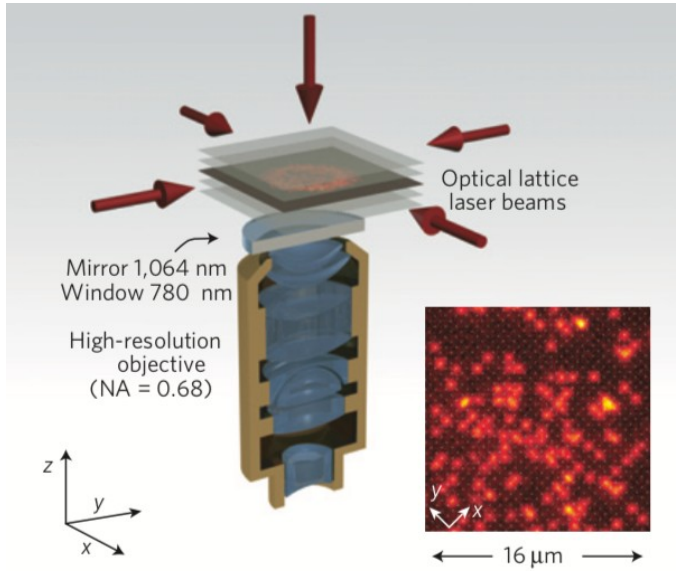

VS

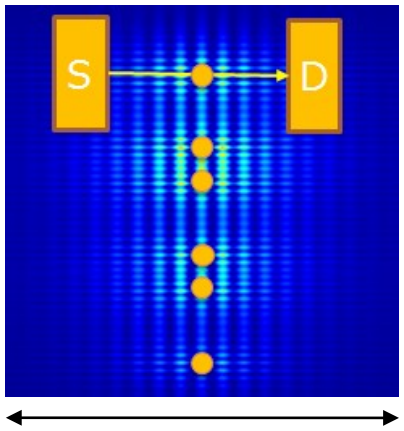

	Cold atoms	Donors
Atomic positions not determined by inter-atomic interactions	Y	Y
Ability to vary lattice spacings dynamically	Y	
Ability to control disorder locally		Y
Scalable to large lattices	Y	(Y)
Freedom from noise	Y	(Y)
Individual readout	Y	(Y)
Access to transport measurements		Y
Long-range Coulomb interactions		Y
Global interference measurements	Y	

Further topological effects

- This shows we can simulate the simplest non-trivial topological model of fermions
- Richer models require further interactions, e.g.
  - Anyons (strong magnetic fields or non-trivial superconducting states)
  - Spin-orbit interactions

Band structure of Si

Conduction band (electrons): derived from s-states, spin-orbit coupling small

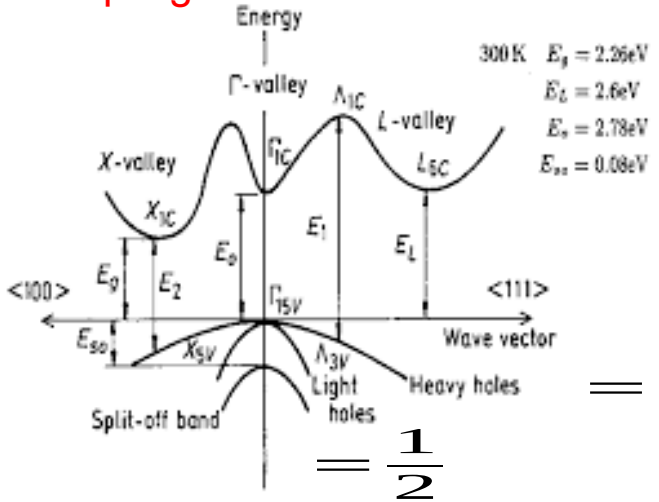

$= \frac{3}{2}$

$= \frac{1}{2}$

Valence band (holes): derived from p-states, strong spin-orbit effects

Opportunities for Group III (acceptor) doping

B deposition by STM lithography using BCl_3 and Si-Cl 'resist'

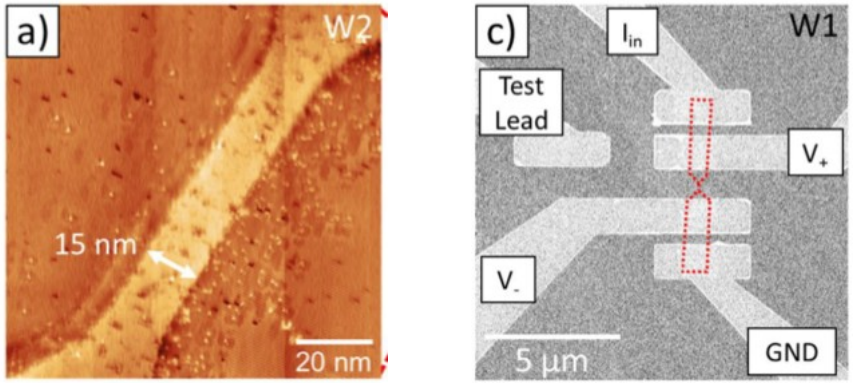

Well-defined nanowires and delta-layers (not yet controlled at single-atom level)

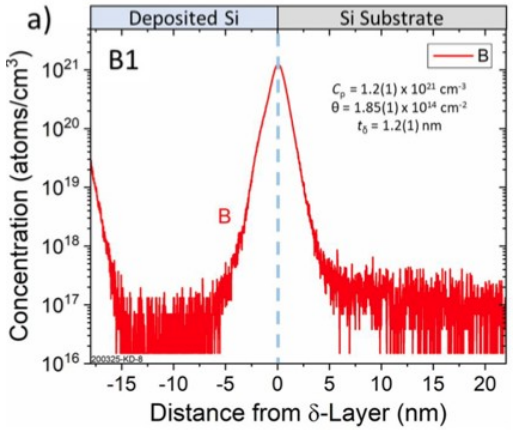

Dwyer *et al. ACS Appl. Mater. Interfaces* **13**, 41275−86 (2021)

Al deposition using $AlCl_3$

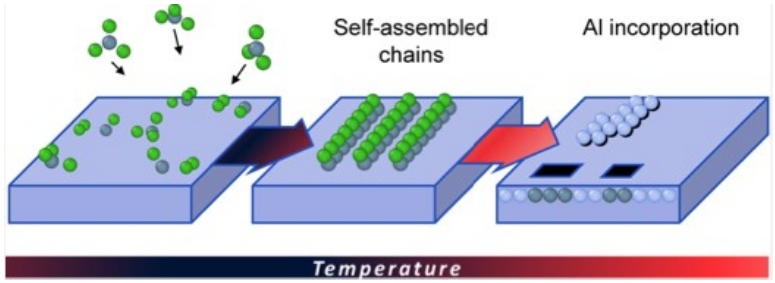

Evidence for AlCl 'chains' and their decomposition to form surface Al

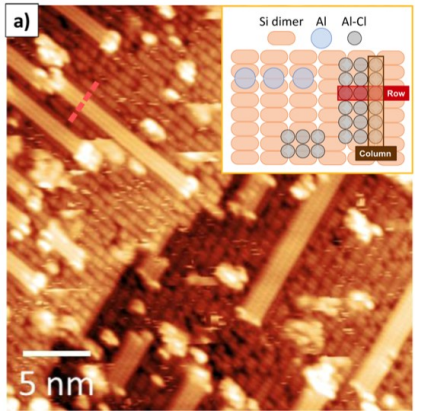

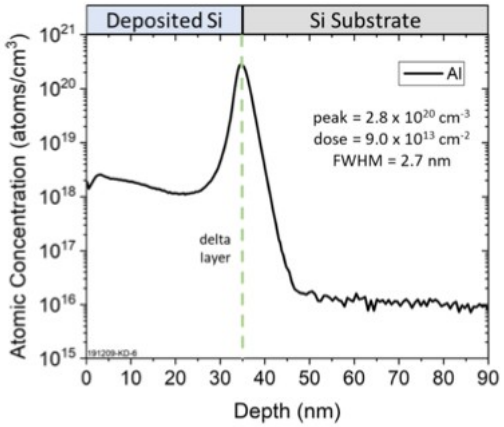

Radu *et al. J. Phys. Chem. C,* **125** 11336−11347 (2021)

Spin-orbit coupling

- Unlike the conduction band, states at the valence-band maximum (-point) are derived from p states having intrinsic (orbital) angular momentum *L*=1
- To quadratic order, cubic symmetry allows only certain combinations of *I* and *k*

$$\hat{H}(\mathbf{k}) = Ak^2 - (A-B)\left(k_x^2 I_x^2 + k_y^2 I_y^2 + k_z^2 I_z^2\right) - \frac{C}{2}\left(\{k_x, k_y\}\{I_x, I_y\} + \{k_y, k_z\}\{I_y, I_z\} + \{k_z, k_x\}\{I_z, I_x\}\right)$$

where

$$\{I_x, I_y\} \equiv I_x I_y + I_y I_x$$

Spin-orbit coupling implies states at valence-band maximum are labelled by , not **I**:

$$\hat{H}(\mathbf{k}) = -\left[\left(\gamma_1 + \frac{5}{2}\gamma_2\right)\frac{k^2}{2m_e} - \frac{\gamma_2}{m_e}\left(k_x^2 J_x^2 + k_y^2 J_y^2 + k_z^2 J_z^2\right) - \frac{\gamma_3}{2m_e}\left(\{k_x, k_y\}\{J_x, J_y\} + \{k_y, k_z\}\{J_y, J_z\} + \{k_z, k_x\}\{J_z, J_x\}\right)\right]$$

The spherical model

Hamiltonian breaks into a spherical part (including the spin-orbit coupling and terms generating heavy-hole light-hole splitting) and non-spherical perturbations

Defining trace-free rank-2 tensors

$$K_{il} \equiv 3k_i k_l - \delta_{il}k^2; \qquad J_{il} \equiv \frac{3}{2}(J_i J_l + J_l J_i) - \delta_{il}J^2$$

the Hamiltonian becomes

$$\hat{H}(\mathbf{k}) = -\left[\frac{\gamma_1}{2m_e}k^2 - \frac{1}{9m_e}\left[\gamma_3 - (\gamma_3 - \gamma_2)\delta_{ik}\right]K_{ik}J_{ik}\right]$$

and the spherical part is

$$\hat{H}(\mathbf{k}) = -\left[\frac{\gamma_1}{2m_e}k^2 - \frac{(3\gamma_3 + 2\gamma_2)}{45m_e}(K^{(2)} \cdot J^{(2)})\right]$$

Scalar product of two rank-2 tensors (rotationally invariant)

In the presence of the potential from a negatively charged (ionized) acceptor at the origin, we obtain

$$-\left[\frac{\gamma_1}{2m_e}p^2 - \frac{(3\gamma_3 + 2\gamma_2)}{45m_e}(P^{(2)} \cdot J^{(2)}) - \frac{e^2}{4\pi\epsilon r}\right]F = \widetilde{E}F$$

Here *F* is a vector of envelope functions satisfying

$$\psi(\mathbf{r}) = \sum_{j\mathbf{k}} F_j(\mathbf{k})\mathrm{e}^{\mathrm{i}\mathbf{k}\cdot\mathbf{r}}\phi_j(\mathbf{k}=0) = \sum_j F_j(\mathbf{r})\phi_j(\mathbf{k}=0)$$

Use zone-centre Bloch functions here, since they are the basis used for

If the envelope function carries orbital angular momentum *L* then is a conserved quantity

Baldareschi and Lipari *Phys Rev B* **8** 2697 (1973)

States of individual acceptors

Need to account for

- Valence-band degeneracy
- Spin-orbit coupling

Spherical model

HH-LH splitting Spin-orbit

$$\hat{H}_s = \frac{p^2}{\hbar^2} - \frac{2}{r} - \frac{\mu}{3\hbar^2}(P^{(2)} \bullet I^{(2)}) + \frac{2}{3}\Delta(\frac{1}{2} - \vec{I} \bullet \vec{S})$$

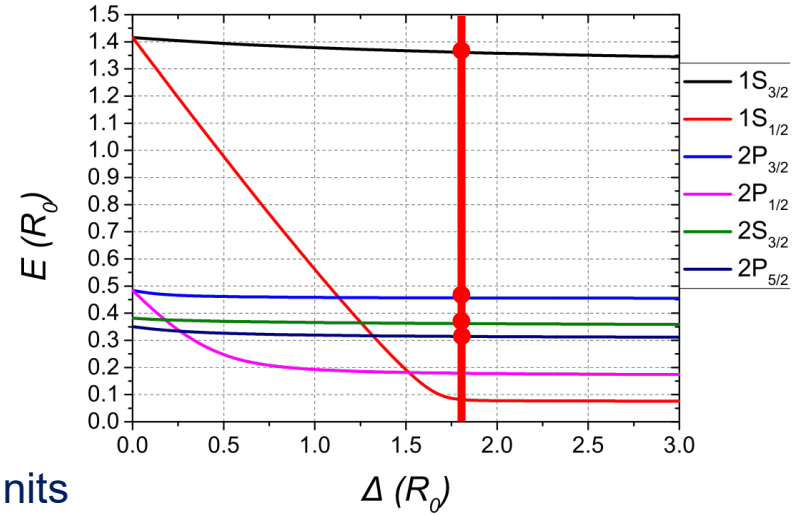

Si

Cubic model

Cubic anisotropy

$$\hat{H}_c = \hat{H}_s + \frac{\delta}{3\hbar^2}([P^{(2)} \times I^{(2)}]_4^{(4)} + \frac{\sqrt{70}}{5}[P^{(2)} \times I^{(2)}]_0^{(4)} + [P^{(2)} \times I^{(2)}]_{-4}^{(4)})$$

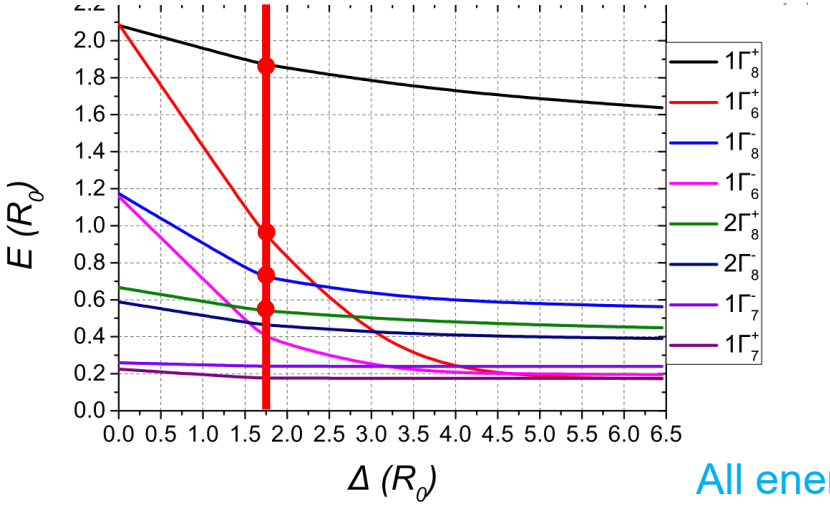

Si

For Si: effective units

Length: =2.55 nm

Energy: =24.8 meV

- Linear combinations of these states provide a basis for calculations of clusters

All energies displayed as electron energies above the valence band, so ground states are at the top!

Finite acceptor chains (along [110])

Large separations: $d_1+d_2=6a_0$

CI total energies, 4-acceptor chain, first 50 states

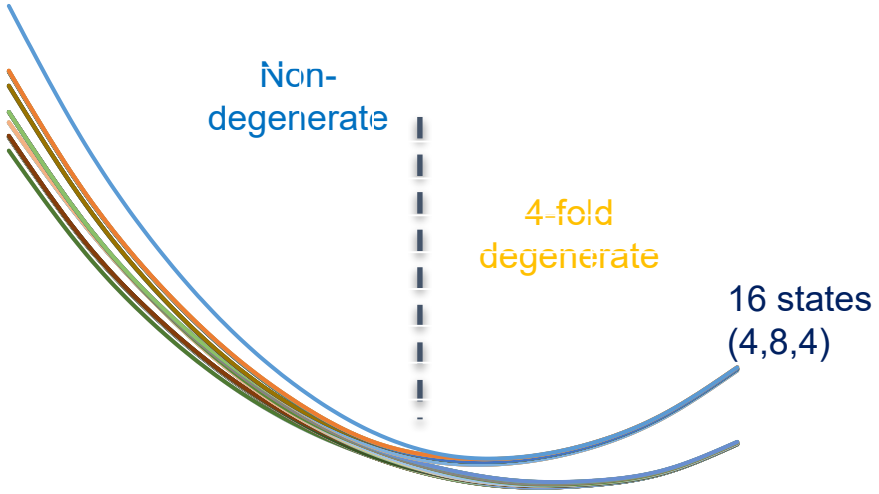

CI, UHF and H-L energies, 4-acceptor chain

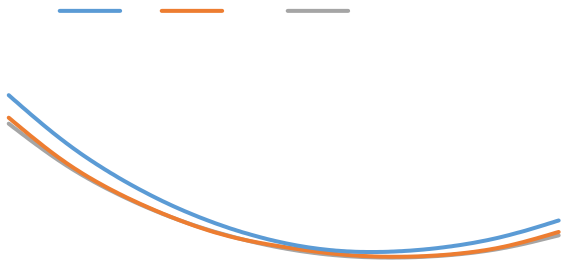

UHF eigenvalues:

4-acceptor chain

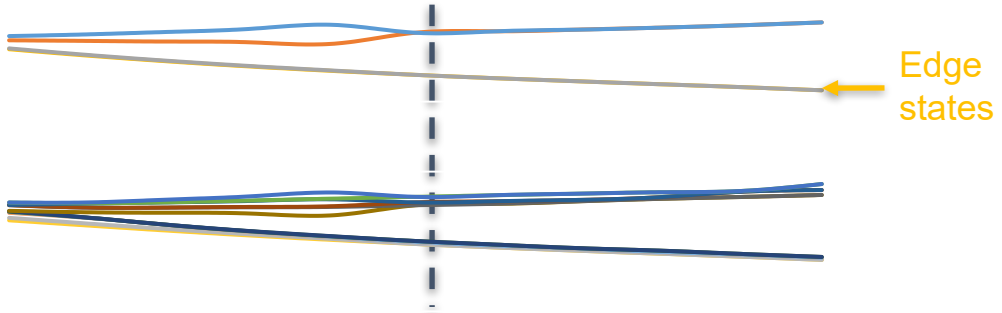

6-acceptor chain

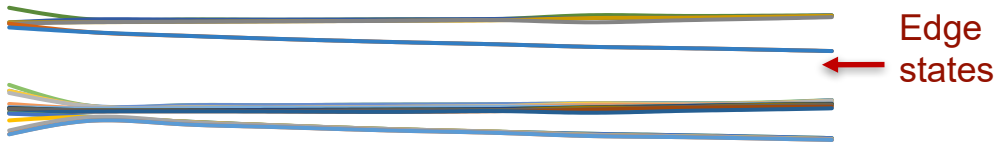

Time-reversal invariant topological insulators

- Insulators that are fundamentally different (in a topological sense) from the vacuum
- Arise when ordering of bands is changed by spin-orbit coupling
- At a surface (interface with non-topoogical vacuum) there must be an odd number of bands of each spin (more generally, odd number of time-reversed pairs) crossing the Fermi energy

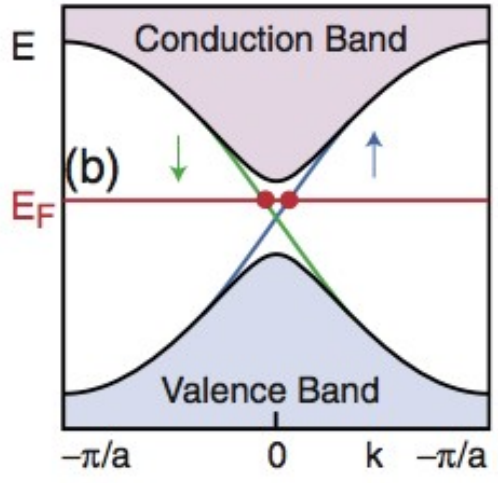

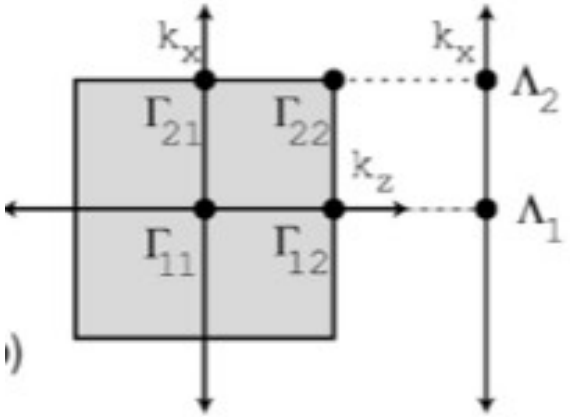

- In 2D there are 4 k-points in the 1BZ which are time-reversal invariant:
- If the material has **inversion symmetry**, can associate with each the product of the parities of each Kramers-degenerate pair of occupied bands

$$\delta_i = \prod_m \xi_{2m}(\Gamma_i)$$

2D Z_2 topological invariant

$$(-1)^\nu = \prod_i \delta_i$$

A surface band pair must join any two projections Λ_a for which products π_a of δ_i differ

Example – graphene and related 2D materials

- Graphene – the original candidate TI

$$\mathcal{H} = \sum_{\langle ij\rangle\alpha} t c^{\dagger}_{i\alpha} c_{j\alpha} + \sum_{\langle\langle ij\rangle\rangle\alpha\beta} i t_2 \nu_{ij} s^{z}_{\alpha\beta} c^{\dagger}_{i\alpha} c_{j\beta}.$$

Nearest-neighbour hopping (produces semi-metallic state)

Spin-orbit coupling (opens 'opposite' gaps at K, K' points)

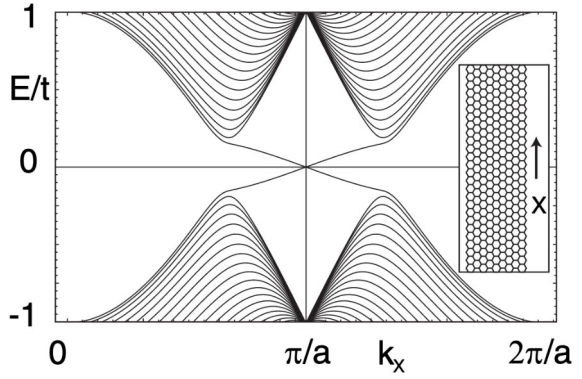

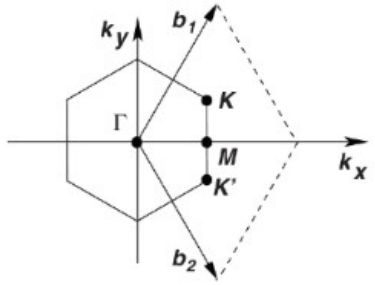

Problem: SOC in C too small to generate significant splittings

Kane and Mele *PRL* **95** 226801 (2005)

- Other honeycomb materials

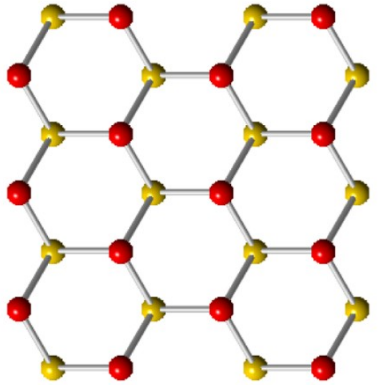

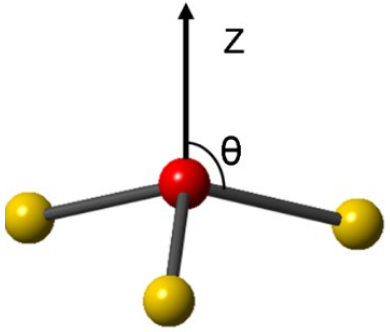

Si, Ge form buckled 2d structures with larger spin-orbit coupling, increasing predicted gap

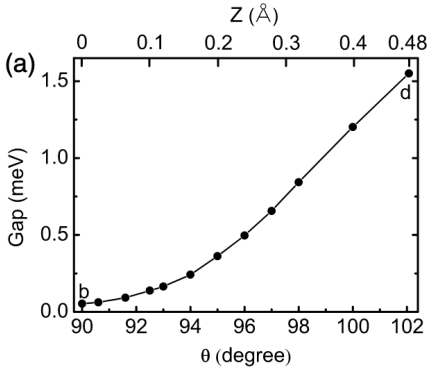

Liu *et al.* PRL **107** 076802 (2011)

The honeycomb acceptor lattice

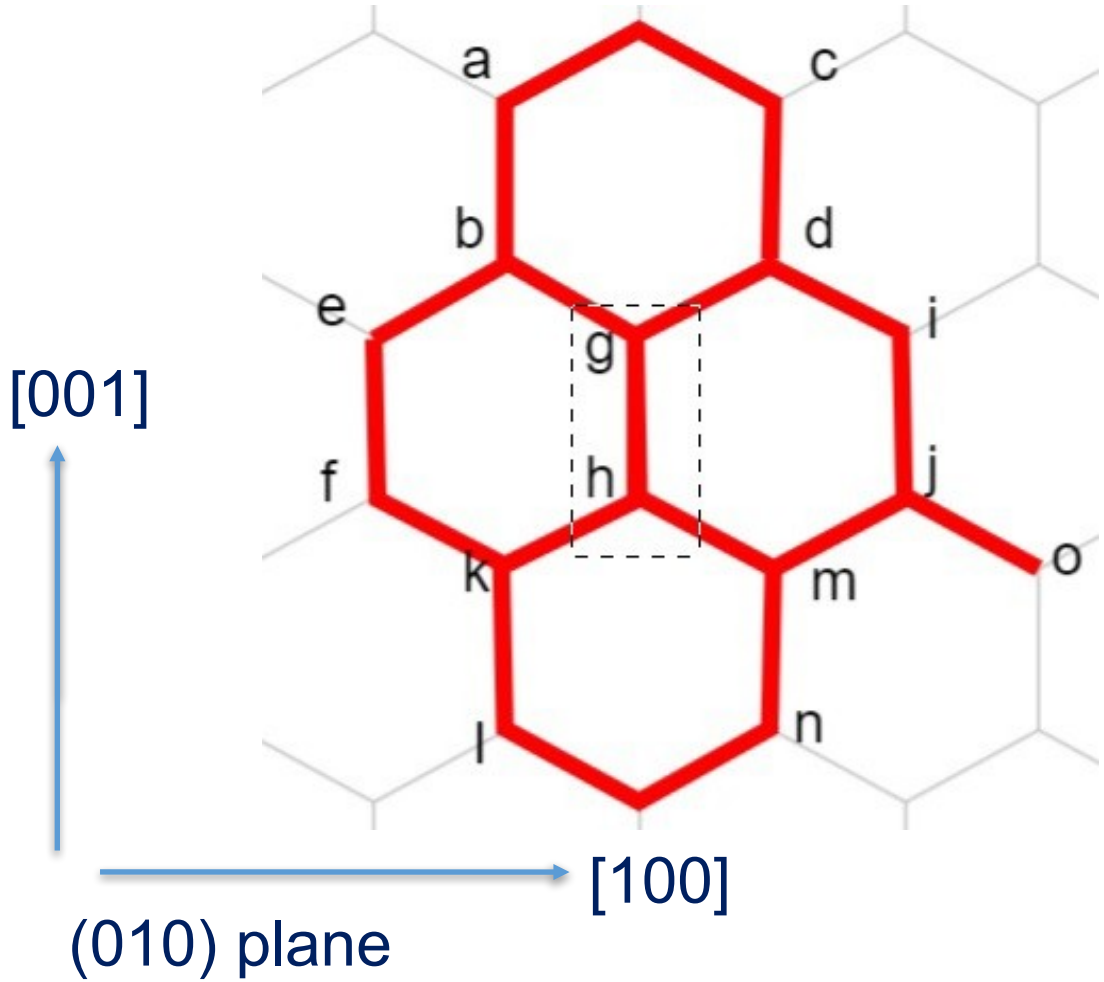

- Graphene-like arrangement of acceptor atoms, two acceptors per unit cell
- Four states on each site:
  - Degenerate in limit of isolated impurity,
  - Formed by spin-orbit coupling
  - Transform like the components of a multiplet

Band structure of excitations

- Spherical model for acceptors (no cubic anisotropy)
- Difference in hopping between and states along each nn bond
- Hopping interaction becomes

$$\hat{H}_{\text{bond } ik} = \sum_{j\in\{3/2,-3/2\}} (t+\delta)(\hat{c}^{\dagger}_{i,j}\hat{c}_{k,j} + \text{h.c.}) + \sum_{j\in\{1/2,-1/2\}} (t-\delta)(\hat{c}^{\dagger}_{i,j}\hat{c}_{k,j} + \text{h.c.})$$

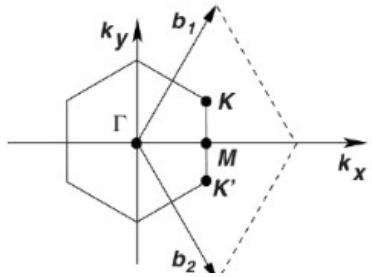

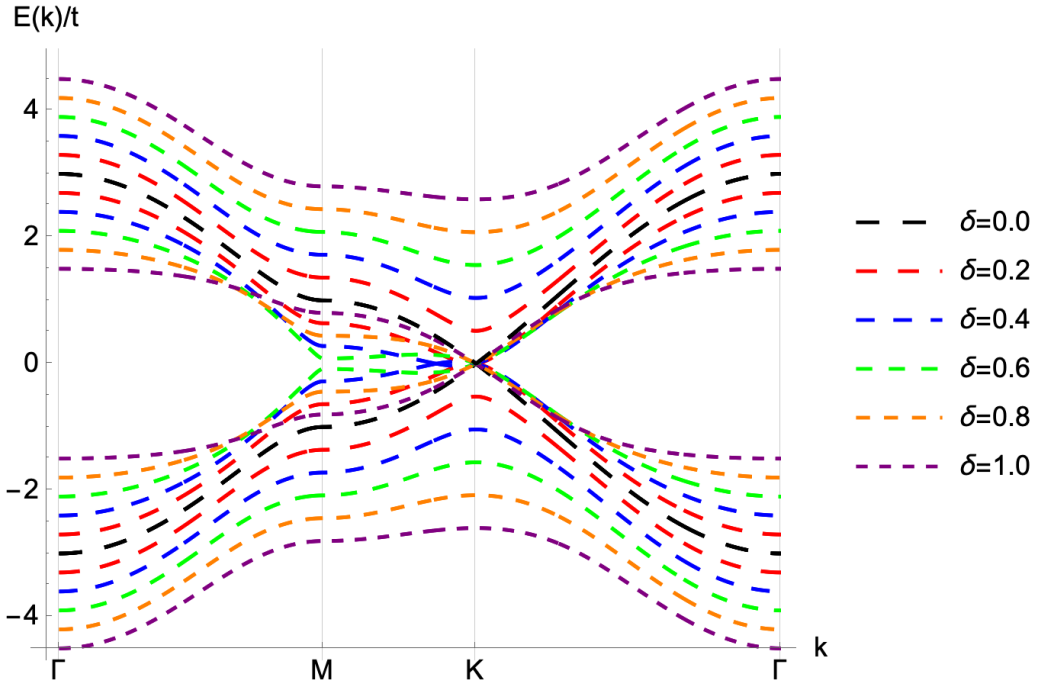

Model is a (topological) insulator beyond a critical value of

A Hubbard-like model

- Spherical model for acceptors (no cubic anisotropy)
- Along each nn bond have hopping

$$\hat{H}_{\text{bond } ik} = \sum_{j\in\{3/2,-3/2\}} (t+\delta)(\hat{c}^{\dagger}_{i,j}\hat{c}_{k,j} + \text{h.c.}) + \sum_{j\in\{1/2,-1/2\}} (t-\delta)(\hat{c}^{\dagger}_{i,j}\hat{c}_{k,j} + \text{h.c.})$$

- On-site Coulomb interaction

$$\hat{H}_{\text{int}} = U \sum_{\text{sites } i} \left(\sum_j \hat{n}_{i,j} \right)^2$$

- Mean-field theory for one hole per acceptor

$$\hat{H}_{\text{MFT}} = U \sum_i \left[\frac{3}{4} - \frac{1}{2} Q_i \hat{Q}_i - \frac{2}{5} m_i \hat{m}_i - \frac{2}{5} p_i \hat{p}_i + (\frac{1}{4} Q_i^2 + \frac{1}{5} m_i^2 + \frac{1}{5} p_i^2) \right]$$

- Mean-field order parameters

$$\hat{Q}_i = \hat{n}_{i,3/2} - \hat{n}_{i,1/2} - \hat{n}_{i,-1/2} + \hat{n}_{i,-3/2} \quad \text{(quadrupole)}$$

$$\hat{m}_i = \frac{3}{2}\hat{n}_{i,3/2} + \frac{1}{2}\hat{n}_{i,1/2} - \frac{1}{2}\hat{n}_{i,-1/2} - \frac{3}{2}\hat{n}_{i,-3/2} \quad \text{(magnetization)}$$

$$\hat{p}_i = \frac{1}{2}\hat{n}_{i,3/2} - \frac{3}{2}\hat{n}_{i,1/2} + \frac{3}{2}\hat{n}_{i,-1/2} - \frac{1}{2}\hat{n}_{i,-3/2}. \quad \text{(3/2-1/2 alignment)}$$

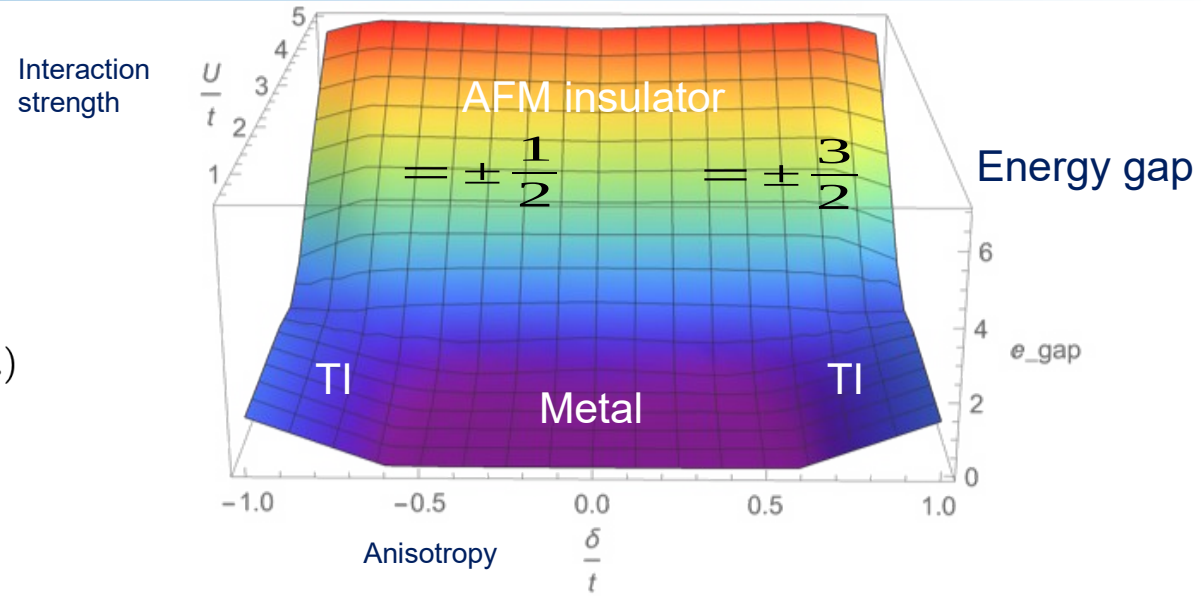

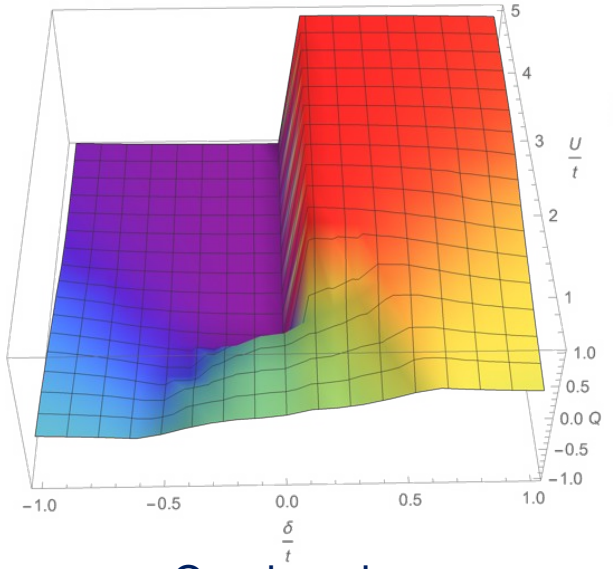

Quadrupole

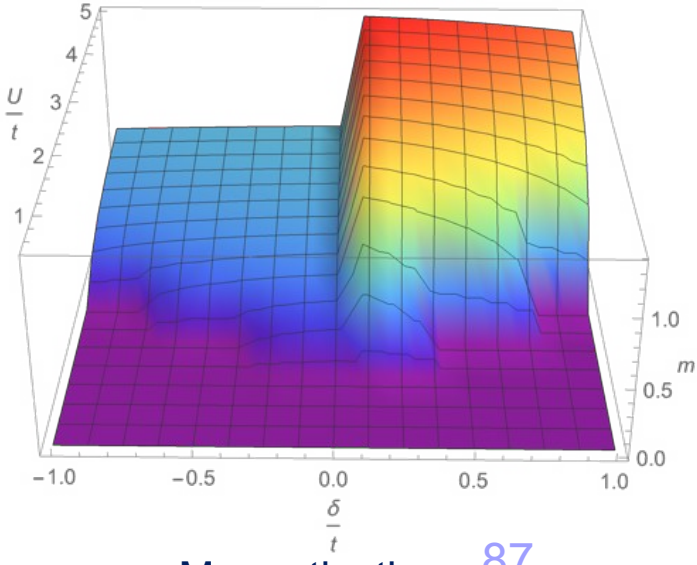

Magnetization

Symmetry of the interactions

Two different routes to create time-reversal invariant topological insulators in the honeycomb lattice:

- Original 'graphene' TI
  - Gap generated by spin-orbit term (spin-dependent hopping between next-nearest neighbours)

$$\hat{H}_{\mathrm{SO}} = \mathrm{i}\lambda \sum_{\langle\langle ij \rangle\rangle} \sum_{\sigma\sigma'} \nu_{ij} \sigma^z_{\sigma,\sigma'} \hat{c}^\dagger_{i\sigma} \hat{c}_{j\sigma'} \quad \text{with} \quad \nu_{ij} = \pm 1$$

  - *Odd* under both reversal of spatial motion and reversal of spins
  - Hence *even* under time-reversal

- 'Acceptor' TI
  - Gap generated by differential hopping along bonds (quadrupole-dependent hopping between nearest neighbours)

$$\hat{H}_{\mathrm{bond}\ ik} = \sum_{j\in\{3/2,-3/2\}} (t+\delta)(\hat{c}^\dagger_{i,j}\hat{c}_{k,j} + \mathrm{h.c.}) + \sum_{j\in\{1/2,-1/2\}} (t-\delta)(\hat{c}^\dagger_{i,j}\hat{c}_{k,j} + \mathrm{h.c.})$$

  - *Even* under both reversal of spatial motion and reversal of spins
  - Hence *even* under time-reversal

Kane and Mele *Phys Rev Lett* **95** 226801 (2005)
Rachel and Le Hur *Phys Rev B* **82** 075106 (2010)

Topological edge states

- Should be able to observe topological edge states directly in the TI phase:

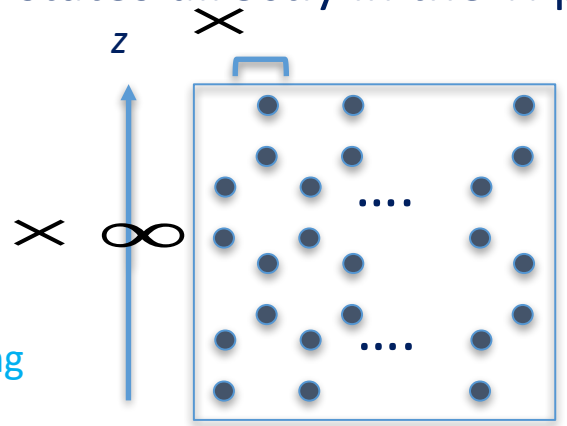

'Armchair' edge

Non-interacting

- Confirmation that the edge states are protected by time reversal symmetry:

Static magnetic order breaks *T* symmetry

Non-magnetic phase

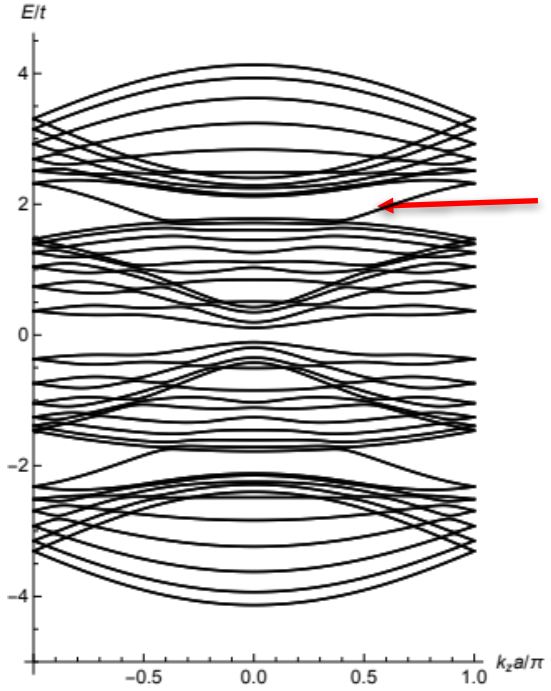

Edge states

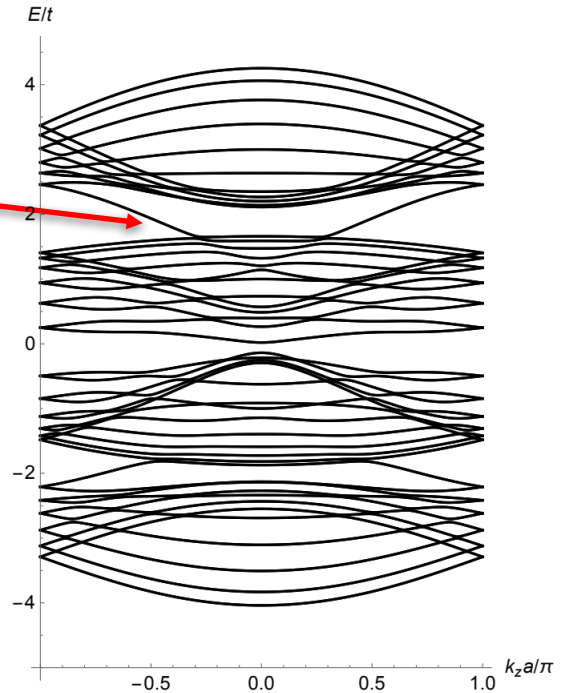

AFM phase

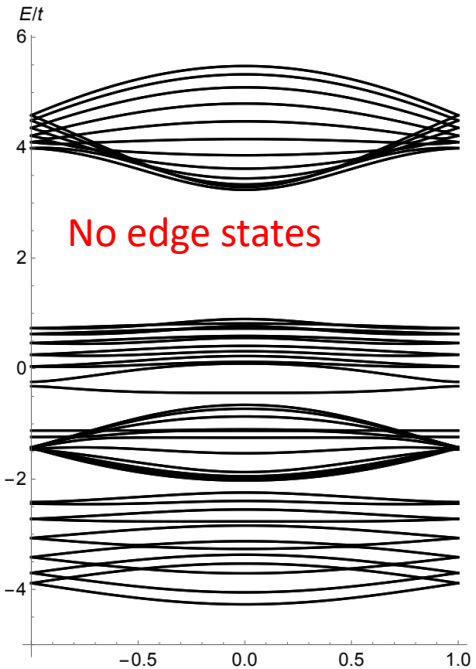

No edge states

Robustness to placement errors

Honeycomb lattice must be distorted to be commensurate with Si growth plane (square symmetry)

Robust region of topological phase around $\{s_1,s_2,s_3\}=\{15,13,8\}$

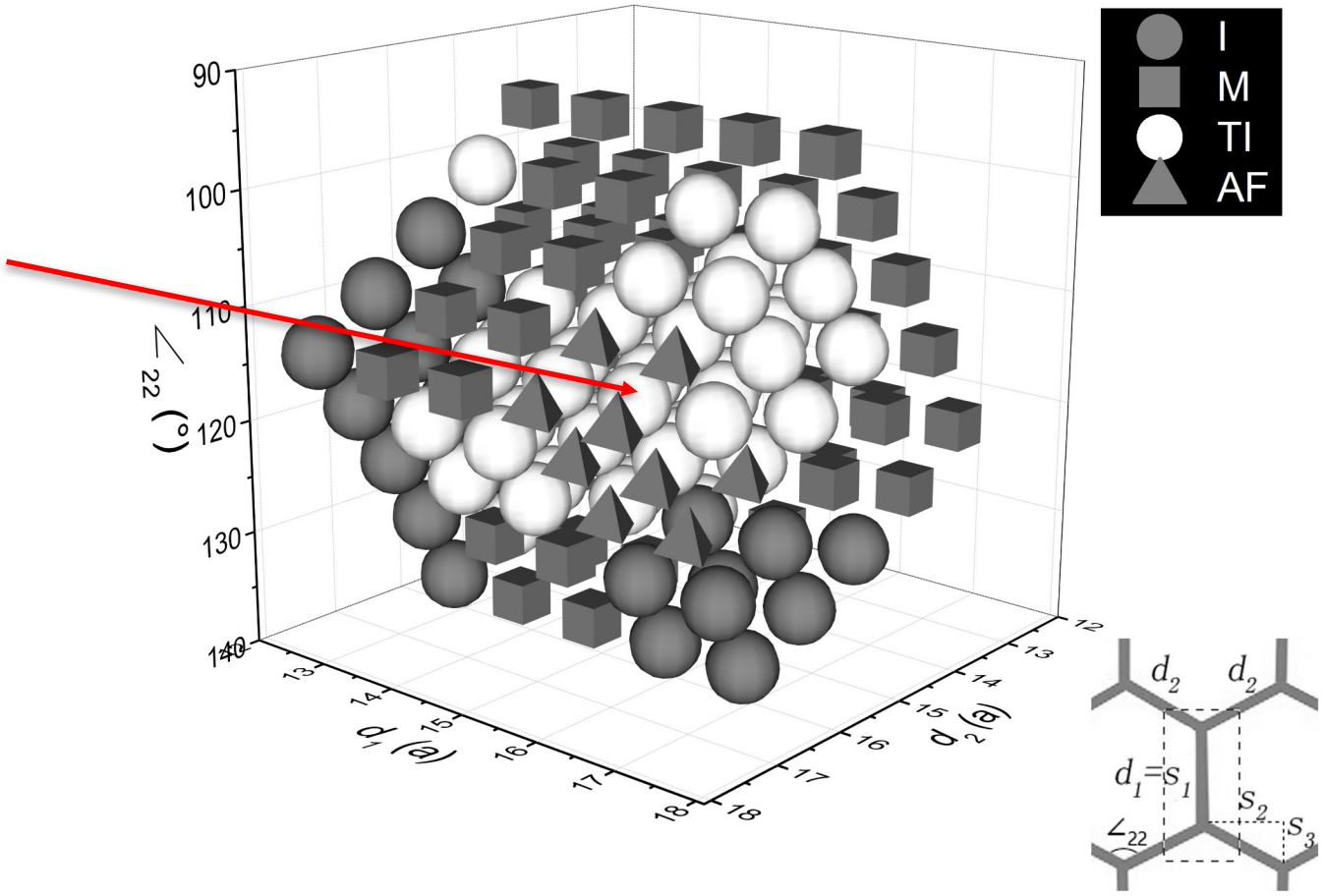

Observation: edge states

- Local density of states of shows regions where all states localized around edges of island
- Predict these should be visible in STM
- Already visible for small islands (e.g. 48 acceptors) but increasingly clear for larger islands

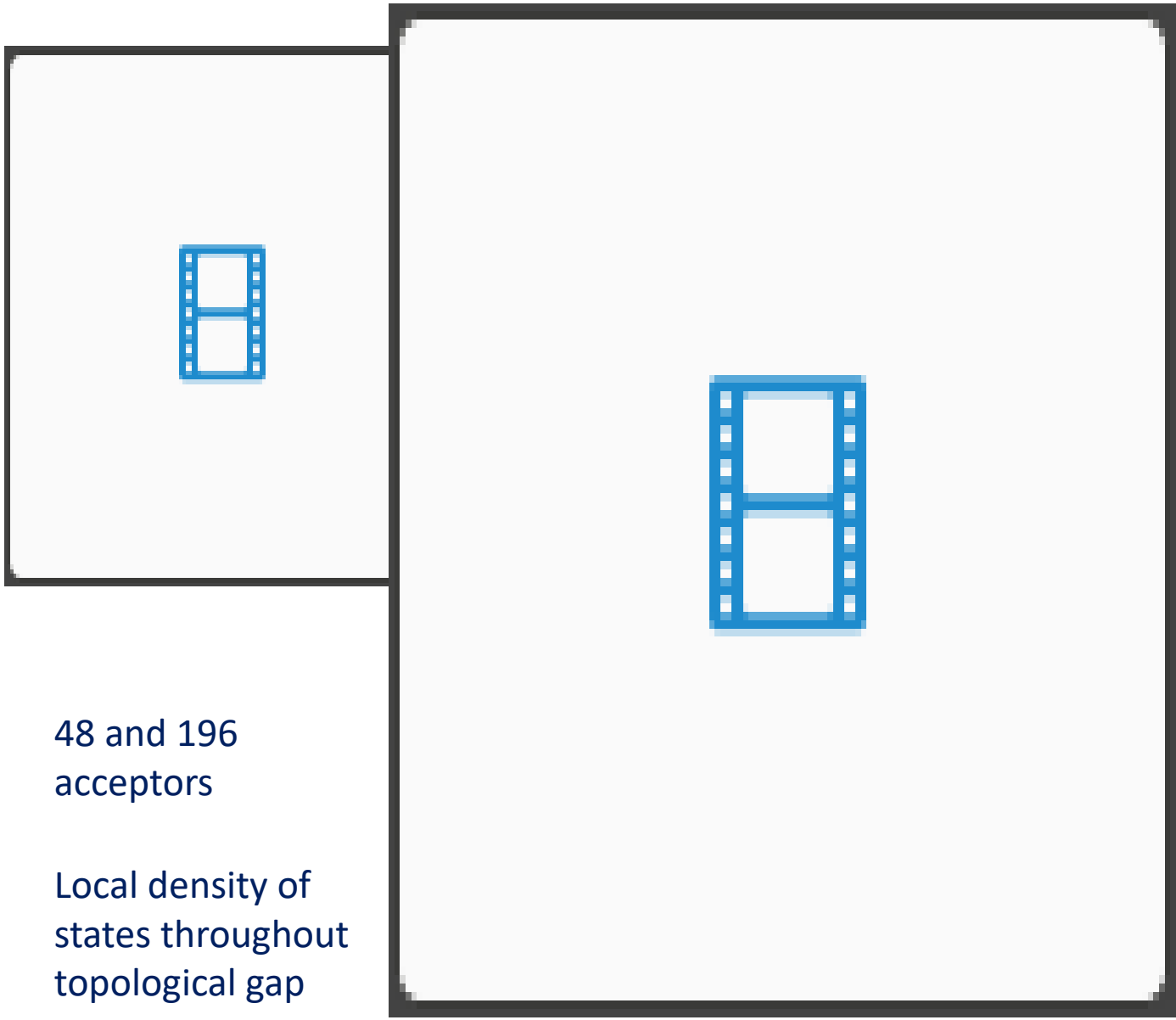

48 and 196 acceptors

Local density of states throughout topological gap

Proposed detection in cold atoms

Challenge: the number of atoms occupying edge states of a TI is often a small fraction of the total

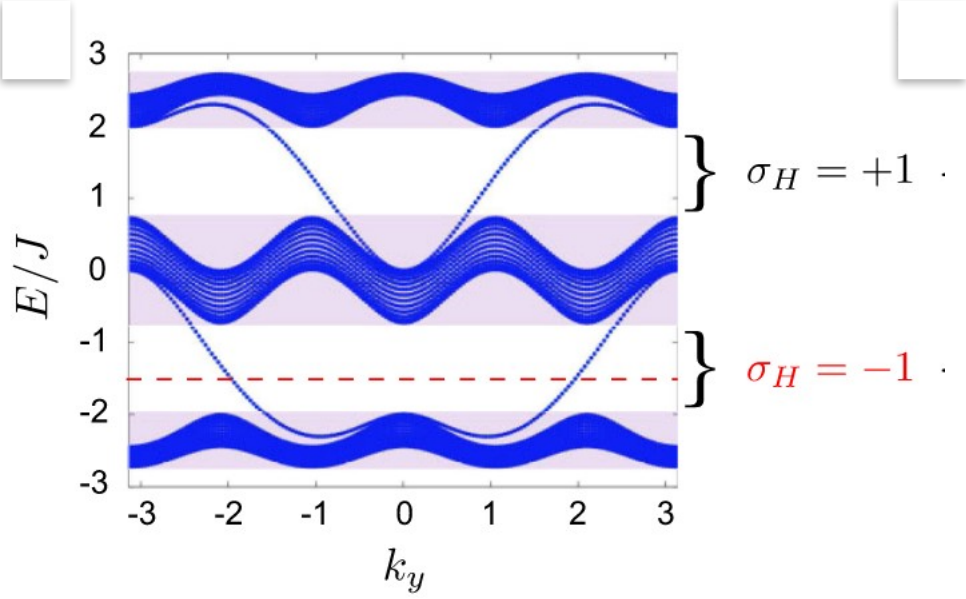

Edge states of a Hoftstadter model (with artificial magnetic flux for neutral atoms) in a cylindrical geometry

Ideas for detection (not so far realised):

Bragg spectroscopy (sensitive to angular momentum): matrix element is

$$I^q_{\alpha\beta} = \frac{1}{2}\int dx\, \psi^*_\alpha(x)\psi_\beta(x) f_L(r) e^{iq\theta}.$$

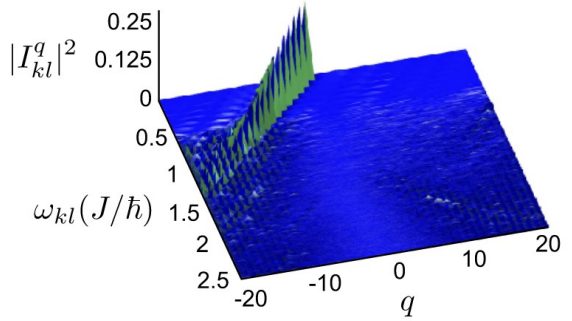

Goldman *et al. Phys Rev Lett.* **108** 255303 (2012)

Direct imaging (combined with propagation of edge states into new regions after a quench and differencing of opposite fluxes)

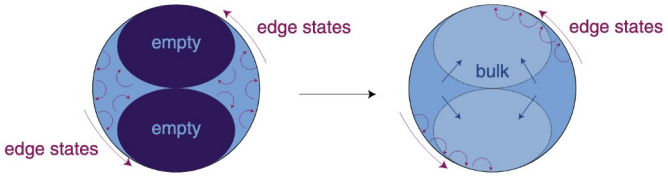

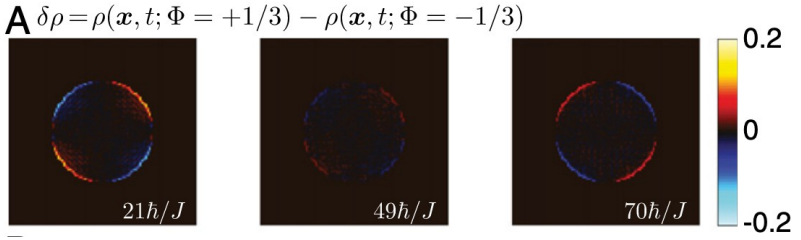

Goldman *et al.* *PNAS* **110** 6736 (2013)

Conclusions

- Donors
  - Charge transfer transitions as dominant low-energy excitations
  - Including multi-valley effects alters the physics and introduces new spin-selective excitations
  - Topological states in dimerized chains have different characters either side of the Mott transition
  - Experimental realizations now possible
- Acceptors
  - Rich spin-orbit physics gives a larger low-energy manifold
  - Correspondingly richer manifolds of topological edge states
  - 2D topological insulator phase produced by spin-orbit coupling
  - Existence of local probes with energy sensitivity gives options for detection
  - Experimental realizations awaited…

mailto:andrew.fisher@ucl.ac.uk

www.london-nano.com

www.compasss.net

Thanks to collaborators

- Wei Wu
- Jianhua Zhu
- Nguyen Le
- Eran Ginossar

University College London

UNIVERSITY OF SURREY

Advanced Technology Institute

- Neil Curson
- Ben Murdin
- Steven Schofield
- Taylor Stock

ADDRESS

Engineering and Physical Sciences Research Council

LCN LONDON CENTRE FOR NANOTECHNOLOGY

UNIVERSITY OF SURREY